# Maintaining structural and functional homeostasis of the *Drosophila* respiratory epithelia requires stress-modulated JAK/STAT activity

Xiao Niu[1, 2], Christine Fink[1], Kimberley Kallsen[3, 4], Leizhi Shi[1, 5], Viktoria Mincheva[1], Sören Franzenburg[6], Ruben Prange[1], Iris Bruchhaus[7], Judith Bossen[1, 8], Holger Heine[2, 8], Thomas Roeder[1, 8]

[1]Kiel University, Zoology, Dept. of Molecular Physiology, Kiel, Germany

[2]Current address: Weifang Medical University, College of Life Science and Technology, Weifang, China

[3]Research Center Borstel – Leibniz Lung Center, Div. of Innate Immunity, Borstel, Germany

[4]Current address: Boehringer Ingelheim, Ingelheim, Germany

[5]Department of Thoracic Surgery, Linyi People's Hospital, Linyi, Shandong, 276000, China

[6]Kiel University, IKMB, Kiel, Germany

[7]Bernhard Nocht Institute for Tropical Medicine, Hamburg, Germany

[8]German Center for Lung Research, Airway Research Center North, Kiel, Germany

18 **Highlights**

19 1. JAK/STAT signaling is active in the entire *Drosophila* respiratory system in all
20 developmental stages.

21 2. The signaling pathway is indispensable for the survival of the tracheal cell.

22 3. Overactivation of the signaling has significant effects on tracheal development and also
23 displays a human disease-associated phenotype in *Drosophila* trachea.

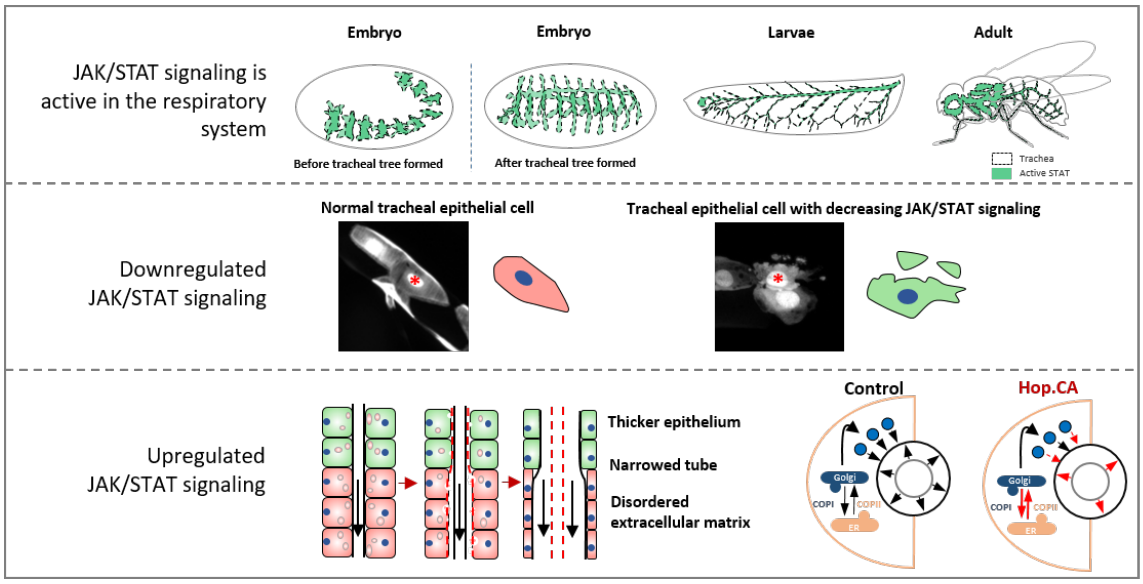


24

25

26

27

## Summary

Signaling mediated by the Janus kinase (JAK)/Signal Transducer and Activator of Transcription (STAT) pathway is critical for maintaining cellular and functional homeostasis in the lung. Thus, chronically activated JAK/STAT signaling is causally associated with lung diseases such as lung cancer, asthma, and chronic obstructive pulmonary disease. To elucidate the molecular processes that transform increased JAK/STAT signaling in airway epithelial cells into the known pathological states, we used a highly simplified model system, the fruit fly *Drosophila melanogaster*. Here, the JAK/STAT pathway is permanently active in almost all airway cells and responds to airborne stressors with increased activity. Silencing of this signaling pathway in epithelial cells resulted in apoptosis. Since the above-mentioned lung diseases are commonly associated with increased JAK/STAT signaling, we assessed this by its ectopic activation in the respiratory epithelium of *Drosophila*. This intervention triggered cell-autonomous structural changes in epithelial cells. These structural changes included phenotypes associated with asthma, namely, thickening of the epithelium, substantial narrowing of the air-conducting space, and impairment of the secretory epicuticular structure of the tracheae. Pharmacological manipulation of JAK/STAT signaling reversed this pathological phenotype. Transcriptomic analyses revealed that several biological processes were affected, which is consistent with the impairment of junction protein trafficking also observed in this study. These results indicate that balanced JAK/STAT signaling is essential for the functionality of the

48 respiratory epithelium and, by extension, the entire organ. In contrast, chronic
49 overactivation of this signaling leads to massive structural changes that are closely
50 associated with pathologies typical of chronic inflammatory lung diseases.

51 **Introduction**

52 The Janus kinase (JAK)/signal transducer and activator of transcription (STAT) signaling
53 system is of central importance for several critical physiological processes such as
54 development, tissue homeostasis, and immune responses (Philips et al., 2022; Rawlings
55 et al., 2004). Signal transduction via this pathway is straightforward and allows
56 environmental factors to directly influence transcriptional activity, linking key biological
57 processes to the environment (Kiu and Nicholson, 2012). Deregulation of this pathway is
58 linked to numerous human diseases, with cancer and inflammatory pathologies being
59 particularly prominent (Hu et al., 2021; Milara et al., 2018). JAK/STAT signaling acts
60 downstream of a plethora of cytokines that transmit immune-related information, acting
61 as a central integration hub in almost all cells of the lung (Yew-Booth et al., 2015)(Villarino
62 et al., 2017). Signaling via this pathway is essential during organ development and for
63 maintaining tissue and immune homeostasis of the fully differentiated lung. Here,
64 JAK/STAT signaling is required to cope with stressors, infection, and damage (Jin et al.,
65 2018; Kida et al., 2008; Major et al., 2020; Makris et al., 2017; Tadokoro et al., 2014). Given
66 the importance of JAK/STAT signaling in the lung, it is predictable that decreased or
67 increased signaling via this pathway leads to pathologies. Whereas reduced JAK/STAT
68 signaling corresponds with impaired repair capacities (Tadokoro et al., 2014), increased
69 JAK/STAT signaling is associated with a plethora of chronic lung diseases including asthma,
70 chronic obstructive pulmonary disease (COPD), idiopathic pulmonary fibrosis (IPF), and

71 lung cancer (Dutta et al., 2014; Georas et al., 2021; Milara *et al.*, 2018; Yew-Booth *et al.*,
72 2015). Despite its simple general organization, the JAK/STAT signaling pathway in
73 vertebrates shows multiple redundancies, parallels, and convergences; a situation that is
74 further complicated since these signaling pathways may act differently in different cell
75 types of the same organ (Hu *et al.*, 2021; Morris et al., 2018; Villarino *et al.*, 2017).
76 Therefore, models with a much simpler JAK/STAT signaling pathway and a less complex
77 cellular composition in the airways should help to elucidate the effects of deregulated
78 JAK/STAT signaling, especially in airway epithelial cells. *Drosophila melanogaster* can be
79 used for this task, as only one receptor (Domeless), one JAK kinase (Hopscotch), and one
80 STAT transcription factor (STAT92E) are present (Arbouzova and Zeidler, 2006; Zeidler and
81 Bausek, 2013). This low level of redundancy offers the unique advantage to study the
82 generic relevance of JAK/STAT signaling. Furthermore, the use of *Drosophila* allows
83 focusing exclusively on the airway epithelium, a resident cell population playing a central
84 role in the orchestration of organ homeostasis, but also for developing chronic pathologies.
85 In the tracheal system of *Drosophila*, the lung's functional equivalent, there is so far only
86 information on the relevance of JAK/STAT signaling during embryonic development and
87 the formation of the adult tracheal system (Brown et al., 2001; Perrimon and Mahowald,
88 1986; Powers and Srivastava, 2019). A lack of JAK/STAT signaling during very early phases
89 of tracheal development impairs tracheal development including cell movement and
90 elongation, as well as invagination processes that lead to tube formation (Brown et al.,

91 2001; Isaac and Andrew, 1996). During the development of the vertebrate lung, very
92 similar processes are operative (Nogueira-Silva et al., 2006; Piairo et al., 2018). In recent
93 years, *Drosophila* served as a model for numerous human diseases (Pandey and Nichols,
94 2011) including those of the lung (Bossen et al., 2021; Levine and Cagan, 2016; Prange et
95 al., 2018; Roeder et al., 2009; Roeder et al., 2012).

96 The current study aimed to elucidate the general importance of JAK/STAT signaling in the
97 airways and understand how chronic deregulation of this pathway in airway epithelial cells
98 results in pathological outcomes. Applying a tailored *Drosophila* model, we could not only
99 show that JAK/STAT signaling is required to prevent apoptosis of airway epithelial cells but
100 that a wide variety of stressors increased signaling via this pathway significantly. Ectopic
101 activation on the other hand, leads to massive structural changes that drastically limit
102 airway epithelial functionality. Using this model, we demonstrated that balanced JAK/STAT
103 signaling in airway epithelia is imperative to prevent the development of pathology and
104 that pharmacological intervention at precisely this point is excellent for addressing it.

105

106 **Results**

107 Activation of the JAK/STAT pathway occurs in a wide variety of organs and can easily and
108 reliably be visualized in *Drosophila* using transcriptional reporters. Here, the activity of the
109 pathway (Fig. 1A) is visualized by a STAT92E-promoter-dependent GFP-based reporter

110 approach (Bach et al., 2007). It was already known that the JAK/STAT pathway is strongly
111 activated in the trachea during embryogenesis and it could be assumed to be important
112 for tracheal development (Bach et al., 2007). However, the exact pattern of its activation
113 is still unclear. To fill this gap of knowledge, we analyzed the *STAT92E*-reporter activity
114 concurrently with *btl>LacZ.nls* (Shiga et al., 1996), which specifically labels the trachea.
115 Activation of the *STAT92E-GFP* reporter was pronounced in a central region in the trachea,
116 mainly in the transverse connective area (Fig. 1B–D). To evaluate if the JAK/STAT pathway
117 also operates in a functional airway epithelium under control conditions, we used the
118 *STAT92E-GFP* reporter line to monitor pathway activity in the larval tracheal system (Fig.
119 1E). JAK/STAT activity was relatively low in the posterior zone of the trachea (Fig. 1F), the
120 tenth tracheal metamere (Tr10), where cells progressively undergo apoptosis in response
121 to trachea metamorphosis (Bosch et al., 2015; Chen and Krasnow, 2014). However,
122 JAK/STAT activity was much stronger in regions such as Tr2, the spiracular branch (SB), and
123 the dorsal branch (DB) than in nearby areas (Fig. 1G and H). In these areas with high
124 JAK/STAT activity, cells re-enter the cell cycle at this developmental stage (Guha et al.,
125 2008; Sato et al., 2008; Weaver and Krasnow, 2008). We next evaluated if JAK/STAT activity
126 is observed in airway epithelial cells of adults. The same approach detected substantial
127 reporter activity in airway epithelial cells of fully developed adults (Fig. 1I). The JAK/STAT
128 pathway was active throughout the entire tracheal system. In addition, we evaluated the
129 expression of the three *upds* in the larval trachea. Experiments using the corresponding

130 enhancer-*Gal4* lines demonstrated that especially *upd2* was highly expressed in the
131 tracheal system (Fig. S1).

132 **The JAK/STAT pathway responds to stressful stimuli**

133 To investigate whether external, stress-associated stimuli can affect JAK/STAT signaling in
134 airway epithelia, we exposed the just-described reporter lines to these stimuli. We
135 focused on airborne stressors and exposed both larvae and adults to them. Here, the
136 administration of cold air (cold), hypoxia, and cigarette smoke (CSE) boosted the activity
137 of the JAK/STAT pathway in airway epithelial cells (Figure 2A and 2C) of both larval and
138 adult animals. A quantitative evaluation of the induced fluorescent signals showed that
139 these increases were statistically significant (Fig. 2C).

140 Then we expanded the analysis of the effects of airborne stressors to include the ligands
141 of the signaling system. We found that one of the three ligands, *upd*, did not show any
142 expression independent of the situation (data not shown). In contrast, the expression of
143 *upd2* and *upd3* were induced by external stimuli, for *upd2* only by CSE, for *upd3* by CSE
144 and hypoxia (Fig. S2). The activity of the *STAT92E-GFP* reporter was induced exactly in the
145 region where also the ligand showed enhanced expression. For further analyses, we
146 focused on the most responsive *upd* gene, namely *upd3*. Expression of *upd3* was low in
147 the tracheal cells of larvae or adult animals that lived under control conditions but could
148 easily be observed in all these tracheal cells when the animals were exposed to external
149 stimuli (Fig. 2B and 2D).

150 **JAK/STAT signaling is essential for the survival of airway epithelial cells**

151 To evaluate the relevance of the JAK/STAT pathway in the *Drosophila* respiratory system,
152 we blocked its activity in the trachea by driving the expression of a dominant-negative
153 isoform of Domeless (*Dome.DN*) using the trachea-specific *btl-Gal4* driver. As a result,
154 some animals developed to the larval stage (Fig. 3A), but all died before reaching the pupal
155 stage. Microscopic analysis of surviving larvae showed that the dorsal trunk (DT) was
156 absent (Fig. 3B'). Time-lapse imaging of embryos experiencing trachea-specific *Dome.DN*
157 expression revealed that all tracheal segments were fused, however, the DT subsequently
158 separated (Fig. 3C). STAT92E-RNAi was used to confirm this kind of effects on trachea. A
159 detailed analysis of the effects caused by constitutive *Dome.DN* expression was performed
160 using a mosaic approach (Wu et al., 2006). Here, driving expression in a mosaic fashion by
161 *vvl-FLP*, *CoinFLP-Gal4* changed the morphology of the affected cells. These cells appear to
162 undergo apoptosis (Fig. 3D). Apoptosis of these affected cells was confirmed by the
163 detection of Dcp1 in exactly these cells, which is a hallmark of apoptosis (Fig. 3E-F).
164 Apoptosis was induced to an even greater extent (and faster) in progenitor cells of the
165 larval tracheal system, where Dcp1-positive cells were observed on day 1 after induction
166 of *Dome.DN* expression (Fig. 3G-I).

167 **Increased JAK/STAT signaling induced cell-autonomous structural changes in epithelial**
168 **cells**

169 We tested the effects of ectopic activation of the JAK/STAT pathway induced by expression
170 of the ligand (*upd3*) or a constitutively active JAK-allele (*Hop.CA*) on tracheal development.
171 These animals died prematurely at the embryo or larval stage (Fig. 4A-B). Microscopic
172 analysis of larvae and embryos showed that the tracheal segment separated at the larval
173 stage (Fig. 4E), however, the disconnection of segments was due to the failure of their
174 fusion at the beginning of tracheal development (Fig. 4C and 4D). In contrast with animals
175 that ectopically expressed *upd3*, more animals expressing *Hop.CA* exhibited an intact
176 tracheal tree (Fig. 4D). However, they all died at the first larval stage, which indicates that
177 JAK/STAT signaling can influence both tracheal formation and growth.

178 To elucidate the effects of JAK/STAT upregulation in the tracheal system, we employed the
179 temperature inducible Gal4/Gal80[ts] system which could initiate activation of the
180 signaling pathway at different time points during larval development (Fig. S3A). We first
181 tested the effects of inhibition of the tracheal JAK/STAT pathway induced by ectopic
182 expression of *Dome.DN* on the animals. Ectopic expression was initiated at three time
183 points during larval development (Fig. S3B). Larval mortality was higher, the earlier
184 expression was initiated. No larvae survived to the pupal stage (Fig. S3C). On the other
185 hand, activation of JAK/STAT signaling induced by ectopic expression of *upd3* or *Hop.CA*
186 led to lower levels of larval death (Fig. S3B). In both cases, no pupae developed into adults
187 (Fig. S3C). Furthermore, we analyzed the effects of this intervention on tracheal structure.
188 Whereas *Dome.DN* overexpression elicited only minor effects on tracheal structure, *upd3*

189 or *Hop.CA* overexpression caused substantial epithelial thickening (Fig. 4F). Quantitative
190 measurements revealed that ectopic overexpression of *Hop.CA* greatly increased
191 epithelial thickness up to more than 10-fold (Fig. 4H). Experiments involving mosaic
192 expression of *Hop.CA* driven by *vvl-FLP*, *CoinFLP-Gal4, UAS-EGFP (vvl-coin)* demonstrated
193 that this effect was cell-autonomous. In the same trachea, cells that expressed *Hop.CA*
194 were much thicker than their neighboring cells that did not express *Hop.CA* (Fig. 4I). The
195 thicker epithelium could be caused by increased cell volume, increased cell number, or
196 reduced tube surface area. To elucidate the mechanisms underlying this structural
197 response, we analyzed the phenotype in more detail. Consequently, the length-thickness
198 (Fig. 4G) product mirrored the findings made when assessing thickness (Fig. 4J). However,
199 the number of cells in the dorsal trunk of Tr8, or DT8 of the trachea with manipulated
200 JAK/STAT signaling was like that in matching controls (Fig. 4K). Hence, the thickening was
201 due to an increase in cell volume, not an increase in cell number. To determine if this
202 thickening is an artifact caused by the isolation method, we directly fixed the trachea *in*
203 *situ* or isolated it in cell culture medium with the same osmolarity as the hemolymph. The
204 same thickening was observed in both cases (Fig. S4). To quantify the time course of this
205 thickening, we subjected the trachea to different treatment regimens prior to analysis. At
206 least 2 days of ectopic expression were necessary to induce this phenotype (Fig. S5).

207 The effects of activating the JAK/STAT pathway on the epithelium were time-dependent
208 (Fig. 4F). To determine if a weaker expression of *Hop.CA* induces similar phenotypes, we

209 used another trachea-specific Gal4-driver, namely, *nach-Gal4* (also called *ppk4-Gal4*). In
210 the *nach-Gal4* line, *Gal4* is expressed from the late embryo stage. Moreover, it is strongly
211 expressed in the early L1 and late L2 stages, at which point expression is stronger than
212 that driven by *btl-Gal4* but is weakly expressed at other larval stages (Liu et al., 2003;
213 Wagner et al., 2009). Microscopic analysis of the trachea showed that weak expression of
214 *Hop.CA* in the trachea promoted epithelial thickening (Fig. 4L). However, epithelial
215 thickening after 4 days of *Hop.CA* induction was lower in *nach>Hop.CA* than in *btl>Hop.CA*
216 (Fig. 4M). On the other hand, weakly driven *upd3* expression in the trachea resulted in
217 identical increases in the thickness as those observed using *btl-Gal4* (Fig. 4N). Finally, we
218 used the same driver to inhibit JAK/STAT signaling in the trachea by expressing *Dome.DN*.
219 Animals died prematurely at the larval stage and their trachea were filled with liquid,
220 demonstrating that functionality was strongly impaired (Fig. 4O). As activation of the IMD
221 pathway by PGRP-LC overexpression induced a very similar phenotype (Wagner et al.,
222 2021), we tested the hypothesis that both, IMD- and JAK/STAT- activation act in the same
223 pathway. Therefore, we activated the IMD-pathway (via PGRP-LC overexpression) while
224 concurrently silencing JAK/STAT signaling (via STAT92e-RNAi) and found no rescue of the
225 thickening phenotype (Fig. 4P).

226 Treatment with various JAK inhibitors (Roskoski, 2016) reversed epithelial thickening
227 induced by ectopic overexpression of *Hop.CA* in the trachea (Fig. 4Q). Treatment with
228 Baricitinib, Oclacitinib, or Filgotinib reduced epithelial thickening by more than 60%

229 therewith showing its potential in interfering with the JAK/STAT signaling pathway and the
230 induced pathological situations (Fig. 4R).

231 **Transcriptomic response to enhanced JAK/STAT signaling**

232 To investigate the molecular mechanisms underlying the effects of chronic JAK/STAT
233 activation on the airways, we performed mRNA-sequencing analysis of tracheal cells
234 expressing *Hop.CA* in third instar larvae. The validity of this experimental procedure was
235 controlled by measuring transcript levels of of *hopscotch* (including *Hop.CA*) and *Socs36E*
236 (one of the best-characterized STAT92E target genes) (Bach et al., 2007), which were
237 upregulated 35-fold and 2.7-fold, respectively ($p < 10^{-12}$) (Fig. S6B). Principal component
238 analysis of biological replicates separated control and overexpression samples into
239 different groups (Fig. S6A, inner region). Finally, the analysis revealed that the expression
240 of 2004 genes was statistically significantly regulated ($p < 0.05$; > 1.5 fold up or down),
241 with 1128 downregulated genes and 876 upregulated genes ($p < 0.05$). A circular heatmap
242 of a subgroup of them under more stringent conditions with 707 differentially expressed
243 genes ($p < 0.01$ and fold change > 2) is shown (Fig. S6A). Moreover, we analyzed changes
244 in expression upon ectopic silencing of the JAK/STAT pathway using *Dome.DN*. A Venn
245 diagram revealed that there was a statistically significant overlap in the cohorts of genes
246 regulated by both interventions (Fisher's exact test, $p < 0.0001$; Fig. S6C).

247 To further elucidate the molecular mechanisms functioning in the thickened epithelium,
248 we performed promotor scan studies and functional enrichment analyses. Genes with the

249 highest rates of induction supported by the lowest p-values were subjected to promoter
250 scanning (Pscan) analysis. Putative genes directly regulated by the JAK/STAT pathway were
251 identified (Tab. 1 and Tab. 2). Among these highly regulated genes, the largest group
252 contained genes that encoded products involved in innate immunity, including seven
253 antimicrobial peptide genes (*IM1 (BomS1), IM2 (BomS2), IM4 (Dso1), IM14 (Dso2),*
254 *CG5791 (BomBc3), CG5778 (BomT3),* and *Drs*). All these antimicrobial peptides, except for
255 Drs, contain one or two CXXC regions. These CXXC-containing peptides belong to the
256 family of Bomanins, whose expression is highly induced following bacterial or fungal
257 infection, and high levels of the corresponding mature peptides are found in the
258 hemolymph of infected flies (Lindsay et al., 2018).

259 Next, we analyzed all significantly regulated genes based on KEGG and GO annotations.
260 Six KEGG pathways and ten categories in GO analysis were enriched in the comparison of
261 the *Hop.CA* expressing trachea compared with the matching controls (Tab. S1 and Fig. 5A-
262 B). One striking feature of the epithelium with chronically activated JAK/STAT signaling
263 was the induced expression of genes involved in “vesicle-mediated transport processes”
264 (Fig. 5A). GO enrichment analysis demonstrated that this term was shared by 32 regulated
265 genes. All these genes were upregulated, except for one (*CG5946*). However, according to
266 a Pscan analysis, these genes did not seem to be direct JAK/STAT targets since predicted
267 STAT92E promoter binding sites were not enriched in the corresponding promoter regions
268 (Tab. S2 and S3). The transcript levels of genes that could be assigned for the term

269 “epicuticle development” were reduced. Here, fifty-five genes relevant to cuticle
270 development were regulated, of which 40 were downregulated. In addition, other
271 biological processes such as “muscle cell differentiation”, “cellular protein-containing
272 complex assembly”, “RNA processing, translation”, and “detection of chemical stimuli”
273 were significantly enriched. In the latter three categories, the number of upregulated
274 genes was like the number of downregulated genes. A schematic representation of the
275 different biological processes superimposed on a scheme of an epithelial cell is shown (Fig.
276 5B). These alterations at the transcript level were reminiscent of the finding in allergic
277 airways disease, where the expression of cell adhesion molecules or their transport to the
278 membrane of airway epithelial cells are impaired (Bonnelykke et al., 2014; Giridhar et al.,
279 2016; Heijink et al., 2020; Xiao et al., 2011). To test this, we analyzed mouse lungs of an
280 experimental asthma model based on the usage of OVA for sensitization (Fig. 5C-E). Those
281 animals of the asthma model displayed typical structural changes in the airways (Fig. 5D)
282 and the relevant proinflammatory cytokines showed the anticipated increase in
283 expression (Fig. 5E). Consistent with the effects observed in *Drosophila*, the expression of
284 genes involved in the biological process vesicle transport were significantly affected in
285 those mice with an induced experimental allergic airway disease (Fig. 5F) and most of
286 these differentially expressed genes were increased.

287 **Impairment of protein transport in airway epithelial cells with chronically enhanced**
288 **JAK/STAT signaling**

289 To evaluate if the transport capacities in the *Drosophila* airway epithelial cells is improved
290 or impaired, we focused on two peripheral membrane-associated proteins involved in
291 cell-cell interactions. These proteins were Coracle (Cora), a component of the septate
292 junctions, and Armadillo (Arm), a component of the adherens junctions. Both proteins
293 depend on vesicle transport to reach their final destinations (Lock and Stow, 2005; Oshima
294 and Fehon, 2011) (Fig. 6A). Immunofluorescence analysis of *Hop.CA*-overexpressing
295 animals revealed that Arm and Cora accumulated in the cytoplasm, which is indicative of
296 dysfunctional vesicle transport (Fig. 6B–E).

297 The transcriptome data revealed that "cuticle development" was another GO that was
298 enriched. This process depends on the secretory abilities of epithelial cells in the larval
299 trachea. Here, chitin-rich structures, called taenidia, are believed to make tubes flexible
300 as well as sufficiently strong in order to avoid collapse (Glasheen et al., 2010). The chitin
301 structure in the trachea showed a strongly reduced degree of regularity in *Hop.CA*-
302 expressing animals compared with control ones (Fig. 7A-B). Chitin staining revealed that
303 the highly organized structure of the chitinous intima was almost completely lost in
304 *Hop.CA*-expressing animals (Fig. 7A'' and 7B''). The mosaic analysis demonstrated that the
305 trachea was structurally disorganized exactly at those sites where *Hop.CA* was expressed
306 (Fig. S7).

307 We propose a simple model that explains structural phenotypes mainly based on the
308 impaired vesicle-mediated transport and the lack of adhesion-associated proteins to the

309 membrane, which is in line with previous findings about this biological process (Jayaram
310 et al., 2008; Tsarouhas et al., 2007) (Fig. 7C). Lumen narrowing is another phenotype that
311 might be caused by the dysfunction of the process which could be observed in our study
312 as well. This is prominently seen when epithelial cells expressed *Hop.CA* at very high levels,
313 as indicated by strong green fluorescence (Fig. 7D-E and Fig. S4).

314

315 **Discussion**

316 The present study aimed to clarify the generic role of the JAK/STAT pathway in the
317 respiratory epithelium. We mainly used the fruit fly *Drosophila* because it has ideal
318 characteristics for conducting this study. The unique features of this model allowed us to
319 focus on the essentials, namely the entirety of the signaling pathway and its importance
320 in respiratory epithelial cells. The JAK/STAT signaling pathway in mammals has a degree of
321 redundancy and parallelism in all its levels, rarely observed in other signaling systems.
322 However, this exceptionally high degree of parallelism hampers determing the significance
323 of JAK/STAT signaling per se and whether it differs substantially from signaling through
324 individual cytokines or receptors. As mentioned earlier, the Drosophila JAK/STAT signaling
325 pathway is simple, allowing targeted manipulation. Here, we showed that 1) JAK/STAT
326 signaling exhibited tonic activity in almost all respiratory epithelial cells, 2) that exposure
327 to airborne stressors such as hypoxia or cigarette smoke enhanced its activity, 3) that
328 blocking JAK/STAT signaling induces apoptosis, and that 4) ectopic activation in epithelial

329 cells induced several phenotypes reminiscent of those found in chronic inflammatory lung
330 diseases such as epithelial thickening or narrowing of the airways. The main results 1-3
331 are thematically very closely related. The tonus of JAK/STAT signaling shown in embryonic,
332 larval, and adult airway epithelia suggests that this cellular function is essential as it
333 probably ensures the survival of these epithelial cells. JAK/STAT signaling is required to
334 maintain the cellular identity of airway epithelial cells (D'Amico et al., 2018) and is
335 important for the response to airway epithelial injury and epithelial cell survival
336 (Juncadella et al., 2013; Paris et al., 2020; Tadokoro *et al.*, 2014). This agrees with our
337 studies, which revealed that blockade of the signaling pathway leads to apoptosis of
338 airway epithelial cells of flies. Furthermore, it implies that the JAK/STAT pathway plays a
339 central role in homeostatic processes in this organ, which also appears to be the case in
340 mammalian airway epithelia. Perturbation of JAK/STAT signaling induces apoptosis in cell
341 lines derived from airway epithelia (Zheng et al., 2016), and this is particularly relevant for
342 tissues and cells that can still divide or grow (Quinton and Mizgerd, 2011). This ability to
343 grow might be one reason for the high susceptibility of Drosophila airway epithelial cells
344 to the blockade of JAK/STAT signaling. Thus, cytokines that activate the JAK/STAT signaling
345 pathway act as survival factors, especially when repair mechanisms are operative.
346 Functional JAK/STAT signaling is also required for regenerative processes after epithelial
347 damage (Kida *et al.*, 2008; Paris *et al.*, 2020; Tadokoro *et al.*, 2014), the response to
348 infections (Matsuzaki et al., 2006), and the reaction to hyperoxia (Hokuto et al., 2004).

349 This indicates that JAK/STAT signaling in mammalian airway epithelial cells and the
350 *Drosophila* trachea is particularly relevant for a protective reaction to stressful stimuli. In
351 *Drosophila*, we observed a basal level of JAK/STAT signaling in these cells, and this
352 signaling was further activated in response to very strong stressors such as chronic
353 exposure to smoke particles. An organ-autonomous JAK/STAT signaling system seems to
354 be operative, composed of the cytokines Upd2 and Upd3 and the activated signaling
355 pathway induced in the same regions of the tracheal system. A comparable, stress-
356 induced system was identified in the intestinal epithelium of flies, where highly stressful
357 insults targeting absorptive enterocytes induce the production and release of the cytokine
358 Upd3 (Jiang et al., 2009; Miguel-Aliaga et al., 2018). In contrast to the intestine, where
359 cytokines produced by stressed enterocytes induce the proliferation of stem cells to
360 replenish the enterocyte pool, stem cells are not involved in the tracheal response.

361 Although a threshold level of JAK/STAT signaling is required for the functionality and
362 survival of airway epithelial cells, excessive activation of this signaling is associated with
363 several lung diseases such as lung cancer, acute lung injury, asthma, pulmonary fibrosis,
364 and COPD (Adnot et al., 2019; Chen et al., 2021; D'Amico *et al.*, 2018; Dutta *et al.*, 2014;
365 Gao et al., 2004; Milara *et al.*, 2018; Parakh et al., 2021; Prele et al., 2012; Simeone-Penney
366 et al., 2007; Yew-Booth *et al.*, 2015; Zhang et al., 2012). The ectopic activation of JAK/STAT
367 signaling in the fly's airway epithelium induced major structural changes, mainly to the
368 architecture of tracheal cells. The mosaic analysis demonstrated that this effect was cell

369 autonomous. These structural changes of the trachea are reminiscent of those observed
370 in asthma, COPD, acute lung injury, and lung cancer. Structural changes that permit
371 fulfillment of the original function of epithelial cells are hallmarks of the epithelial-to-
372 mesenchymal transition. In lung cancer, the epithelial-to-mesenchymal transition
373 depends on JAK/STAT signaling (Liu et al., 2014).

374 Ectopic JAK/STAT pathway activation also induced complex transcriptomic alterations in
375 airway epithelial cells. These changes also affected immune-relevant genes, such as those
376 encoding antimicrobial peptides, mainly from the Bomanin family. This dependency of
377 antimicrobial responses on JAK/STAT signaling is also seen in the mammalian airway
378 epithelium (Choi et al., 2013; Simeone-Penney *et al.*, 2007). However, chronically
379 activated JAK/STAT signaling perturbed secretory processes and the formation of
380 extracellular structures. The extracellular matrix defects caused by *Hop.CA* overexpression
381 are reminiscent of the pathophysiology of the aforementioned chronic lung diseases that
382 involve responses to acute or chronic injury (Fahy and Dickey, 2010). Therefore, attempts
383 to enhance the repair capacities of epithelial cells by inducing structural changes via
384 excessive JAK/STAT signaling would also perturb normal cellular functions, such as the
385 transport of junction proteins to the membrane. This would lead to a reduced barrier
386 function of the epithelium, which is a hallmark of chronic lung diseases such as asthma
387 and COPD (Georas and Rezaee, 2014; Gon and Hashimoto, 2018; Heijink et al., 2012). We

388 also observed epicuticular changes, which considerably influenced the structure of the
389 whole organ. However, it is difficult to identify an equivalent response in vertebrates.

390 Furthermore, our finding that the JAK/STAT signaling pathway operates in airway epithelial
391 cells of embryos, larvae, and adults implies that it plays a central role in these cells at all
392 developmental stages. The JAK/STAT pathway is involved in the embryonic development
393 of the tracheal system (Hombria and Sotillos, 2013). We clarified the sequence of
394 developmental steps in which this signaling pathway plays a central role. The JAK/STAT
395 signaling pathway is particularly relevant for developing and maintaining the dorsal trunk.
396 It is a matter of debate, whether JAK/STAT signaling is essential for mammalian lung
397 development. However, the prevailing view that JAK/STAT signaling is not essential for
398 embryonic lung development (Tadokoro et al., 2014) has been challenged by recent
399 studies (Piairo et al., 2018). Although JAK/STAT signaling is essential for different aspects
400 of tracheal development, the major focus of the current study was to understand its role
401 in maintaining homeostasis in the fully functional airway epithelium.

402 The JAK/STAT pathway is an excellent target for therapeutic intervention in many lung
403 diseases, including asthma, COPD, acute lung injury, idiopathic pulmonary fibrosis, and
404 lung cancer (Athari, 2019; Loh et al., 2019; Milara *et al.*, 2018; Severgnini et al., 2004; Song
405 et al., 2011; Yew-Booth *et al.*, 2015). We demonstrated that pharmacological interference
406 of the JAK/STAT signaling pathway reverted the structural phenotype observed upon
407 ectopic activation of this signaling and, consequently flies survived. This shows that the

408 *Drosophila* model is not only suitable to study the structural effects of excessive JAK/STAT
409 signaling and the underlying molecular mechanisms but also to screen compounds and
410 thereby identify novel therapeutic strategies. Moreover, the intrinsic architecture of the
411 *Drosophila* system allows the prediction that the major site of action is the airway
412 epithelium, thus implying that inhalation would be the ideal route of drug administration
413 in a therapeutic setting.

414 It should be remembered that the vertebrate lung and insect trachea are not homologous.
415 Nevertheless, both airway systems share a high degree of similarity regarding their
416 development, physiology, innate immunity, and operative signaling systems (Andrew and
417 Ewald, 2010; Bergman et al., 2017). Therefore, the fruit fly is a valuable tool for studying
418 genes associated with a great variety of chronic lung diseases, including asthma, COPD,
419 and lung cancer (Bossen et al., 2019; Kallsen et al., 2015; Levine and Cagan, 2016; Prange
420 *et al.*, 2018; Roeder *et al.*, 2009; Roeder *et al.*, 2012). This simple model can be used as
421 part of an experimental toolbox to elucidate the role of JAK/STAT signaling in the airways
422 and the effects of chronic deregulation of this signaling. In addition, it provides a readily
423 accessible experimental system that is amenable to pharmacologic interventions and
424 allows hypotheses and intervention strategies to be easily tested.

425

426 **Material and Methods**

427 ***Drosophila* strains and husbandry**

428 *STAT92E-GFP* was used to monitor the activation of the pathway (Bach et al., 2007); the
429 Gal4-UAS system (Brand and Perrimon, 1993) was used to target ectopic expression to the
430 tracheal system. Gal4 drivers used were: *btl-Gal4, UAS-GFP* on the 3rd chromosome, and
431 *btl-Gal4, UAS-GFP* on the 2nd chromosome (obtained from the Leptin group, Heidelberg,
432 Germany); *upd2-Gal4*; *upd3-Gal4* (Prange et al., 2018); *nach-Gal4* (Liu et al., 2003). The
433 UAS responders included: *UAS-LacZ.nls* (BDSC 3956), *UAS-domeΔcyt2.1* (*UAS-Dome.DN*)
434 and *UAS-Hop.CA* (*UAS-hopTumL*) were obtained from N. Perrimon (Brown et al., 2001;
435 Harrison et al., 1995). The *UAS-upd3* was constructed in our lab. *TubP-Gal80[ts]* (BDSC
436 7018) was obtained from the Bloomington stock center. Unless otherwise stated, the flies
437 were raised on standard medium at 25 °C with 50–60% relative humidity under a 12:12 h
438 light/dark cycle as described earlier (Fink et al., 2016).

439 **Coin-FLP expression system**

440 *Vvl-FLP/CyO; btl-moe.mRFP* (BDSC 64233), *tubP-Gal80[ts]* and *CoinFLP-Gal4, UAS-2xEGFP*
441 (BDSC 58751) were used to construct animals for the tracheal mosaic analysis. Ventral
442 veins lacking (*vvl*) was expressed in larval tracheal clones that covered approximately 30
443 to 80% of the trachea (Bosch *et al.*, 2015; Chen and Krasnow, 2014). The genotype of the
444 flies was *vvl-FLP*, *CoinFLP-Gal4*, *UAS-2xEGFP/CyO* (*vvl-coin*) and *vvl-FLP*, *CoinFLP-Gal4*,
445 *UAS-2xEGFP/CyO*; *tub-Gal80[ts]* (*vvl-coin.ts*).

446 **Developmental viability**

447 For developmental viability of eggs, the eggs were collected overnight and were not
448 physically handled in any way. The number of the hatched eggs and the pupae were
449 counted starting from two days after the collection. Each group has 4 replicates that
450 included more than 20 eggs. For developmental viability of larvae, *tub-Gal80[ts]* was used
451 to limit UAS responder expression at the larvae stage. Animals were raised at 18 °C to keep
452 the UAS responder gene silent. Larvae at different instar stages were transferred to a new
453 medium at 29 °C. In this study, usually 4 replicates were performed with 30 larvae. The
454 stage of larvae was determined via the appearance of anterior spiracles.

455 **Determination of epithelial thickness**

456 The trachea of L2 and L3 Larvae were carefully dissected from the posterior side of the
457 body in PBS. The isolated trachea were immersed in 50% glycerol and digital images were
458 captured within 15 min. L2 Larvae were distinguished from L3 larvae by the appearance
459 of anterior spiracles. The relative ages of L3 larvae were inferred from the size of the
460 animal. 30 larvae were used in each group and specimens were analyzed by Image J.

461 **Drug application in *Drosophila***

462 JAK inhibitors (Baricitinib #16707, Oclacitinib #18722, Filgotinib #17669 - Cayman
463 Chemicals, Michigan, USA) were diluted in DMSO [100 mM]. For later application the
464 inhibitors were diluted 1:10 in 100% EtOH. We used 20 µl of each diluted inhibitor for 2

465 ml of concentrated medium (5% yeast extract, 5% corn flour, 5% sucrose, 1% low-melt
466 agarose, 1 ml of 10% propionic acid and 3 ml of 10% Nipagin). The eggs of each crossing
467 have been applicated on the modified medium and kept at 20 °C until the larvae reach
468 the L2 stage. Afterwards they were incubated at 30 °C for 2 days to induce the *btl-Gal4,*
469 *UAS-GFP; tub-Gal80[ts]* (*btl.ts*)–driver. The trachea of L3 Larvae were carefully dissected
470 from the posterior side of the body in PBS. Isolated trachea was immersed in 50% glycerol
471 and digital images were captured in 15 min. 10 larvae were used for each group.

472

473 **Experimental design for hypersensitivity pneumonitis in mice**

474 Experimental design for hypersensitivity pneumonitis contains two processes,
475 sensitization and challenge of mice with ovalbumin (Sigma Aldrich, A5503). The protocol
476 refers to the protocol that (Daubeuf and Frossard, 2013) described with a few
477 modifications. 8 week-old Balb/C mice were sensitized with intraperitoneal injections of
478 20 μg of OVA emulsified in aluminum hydroxide in a total volume of 1 ml on days 7 and
479 14, followed by 3 consecutive challenges each day by exposure to OVA or PBS aerosol for
480 30 min. Mice were sacrificed 24 h following the final challenge. The left lungs were
481 collected for histological analysis and the superior lobes were dissected for RNA analysis.
482 6 mice per group were used in this experiment and 4 mice were randomly selected in
483 each group for analyses. Total mRNA sequencing, data processing, and statistical analysis
484 were performed by Genesky (Shanghai, China). The experimental protocols were

485 approved by the Animal Care and Protection Committee of Weifang Medical University
486 (2021SDL418).

487 **AB-PAS staining and immunofluorescence analysis of mouse lung**

488 Mice were sacrificed in excess $CO_2$ gas. The lungs of euthanized mice were inflated by
489 intratracheal injection of cold 4% paraformaldehyde and then were fixed and embedded
490 in paraffin as described in (Baligar et al., 2016). AB-PAS staining, and Immunofluorescence
491 analysis were supported by Servicebio (Wuhan, China). All sections were photographed
492 using a microscope slide scanner (Pannoramic MIDI: 3Dhistech). The materials and
493 methods could be found at the following link https://www.servicebio.cn/data-
494 detail?id=3040&code=MYYGSYBG and https://www.servicebio.cn/data-detail?id=35
495 95&code=RSSYBG. We list the main reagents here: AB-PAS solution set (Servicebio,
496 G1049), Anti-CD11b (Servicebio, GB11058) and DAPI (Servicebio, G1012-10ML).

497 **Time-lapse microscopy**

498 All images were acquired using a ZEISS Axio Image Z1 and a ZEISS LSM 880 fluorescent
499 microscope (INST 257/591-1 FUGG). Embryos were dechorionated in 3% sodium
500 hypochlorite and immersed in Halocarbon oil 700 (Sigma Aldrich, 9002-83-9). Then the
501 embryos were imaged after stage 15 when the tracheal tree formed at 3 hours intervals.
502 40 embryos were investigated in each group.

503 **Cigarette smoke and hypoxic exposure**

504 All cigarette smoke exposure experiments were carried out in a smoking chamber,
505 attached to a diaphragm pump. Common research 3R4F cigarettes (CTRP, Kentucky
506 University, Lexington, USA) were used for all experiments. The vials containing animals
507 were capped with a monitoring grid to allow the cigarette smoke to diffuse into the vial.
508 For long-time smoke experiments, L2 larvae were exposed to smoke three times a day for
509 30 min each, on two consecutive days. For heavy smoke experiments, L3 larvae were
510 exposed to smoke of 2 cigarettes for 45 min, which led to about 35-50% mortality. To study
511 the effects of hypoxia on the activity of JAK/STAT signaling pathway, larvae were exposed
512 to long-term hypoxia and short-term hypoxia separately. For long-term hypoxia
513 experiments, L2 larvae were exposed to 5% oxygen three times a day for 30 min each, on
514 two consecutive days. For short-term hypoxia experiments, L3 larvae were exposed to 1%
515 oxygen once for 5 hours. At least 20 animals in 4 vials were investigated in each group.

516 **Immunohistochemistry of *Drosophila* trachea**

517 Larvae were dissected by ventral filleting and fixed in 4% paraformaldehyde for 30 min.
518 Embryos were staged according to Campos-Ortega and Hartenstein (Campos-Ortega and
519 Hartenstein, 1997) and fixed in 4% formaldehyde for 30 min. Immunostaining followed
520 standard protocols as described earlier (Jeon et al., 2008; Levi et al., 2006). GFP signals
521 were amplified by immunostaining with polyclonal rabbit anti-GFP (used at 1:500, Sigma-
522 Aldrich, Merck KGaA, Darmstadt, Germany, SAB4301138). 40-1a (used at 1:50, DSHB, Iowa
523 City, USA) was used to detect Beta-galactosidase. Coracle protein was detected with a

524 monoclonal mouse anti-coracle antibody (used at 1:200, DSHB, Iowa City, USA, C566.9).
525 Armadillo protein was detected with a monoclonal mouse anti-armadillo antibody (DSHB,
526 US, N2 7A1, used at 1:500). A monoclonal rabbit Cleaved Drosophila Dcp1 (used at 1:200,
527 Cell Signaling, Frankfurt/M, Germany, #9578) was used to detect apoptotic cells.
528 Secondary antibodies used were: Cy3-conjugated goat-anti-mouse, Cy3-conjugated goat-
529 anti-rabbit, Alexa488-conjugated goat-anti-mouse (used at 1:500, Jackson
530 Immunoresearch, Dianova, Hamburg, Germany), Alexa488-conjugated goat-anti-rabbit
531 (used at 1:500, Cell signaling, Frankfurt/M, Germany, #9578). Tracheal chitin was stained
532 with 505 star conjugated chitin-binding probe (NEB, Frankfurt/M, Germany, used at 1:300).
533 Nuclei were stained with 4',6-Diamidino-2-Phenylindole, Dihydrochloride (DAPI) (Roth,
534 Karlsruhe, Germany, 6843). 30 specimens were investigated in each group. Specimens
535 were analyzed and digital images were captured either with a confocal (Zeiss LSM 880,
536 Oberkochen, Germany) or a conventional fluorescence microscope (ZEISS Axio Imager Z1,
537 Zeiss, Oberkochen, Germany), respectively.

538 **RNA isolation and RNA sequencing**

539 For the gene expression analysis of 3rd instar larvae trachea, animals were dissected in
540 cold PBS and isolated trachea transferred to RNA Magic (BioBudget, Krefeld, Germany)
541 and processed essentially as described earlier (Prange et al., 2018) with slight
542 modifications. The tissue was homogenized in a Bead Ruptor 24 (BioLab products,
543 Bebensee, Germany) and the RNA was extracted by using the PureLink RNA Mini Kit

544 (Thermo Fisher, Waltham, MA, USA) for phase separation with the RNA Magic reagent. An
545 additional DNase treatment was performed following the on-column PureLink DNase
546 treatment protocol (Thermo Fisher, Waltham, MA, USA).

547 Sequencing libraries were constructed using the TruSeq stranded mRNA kit (Illumina, San
548 Diego, USA) and 50 bp single-read sequencing was performed on an Illumina HiSeq 4000
549 with 16 samples per lane. Resulting sequencing reads were trimmed for low-quality bases
550 and adapters using the fastq Illumina filter (http://cancan.cshl.edu/labmembers/gordon
551 /fastq_illumina_filter/) and cutadapt (version 1.8.1) (Martin, 2011). Transcriptomics
552 analysis including gene expression values and differential expression analysis was done
553 using CLC Genomics Workbench. The detailed protocols can be obtained from the CLC
554 Web site (http://www. clcbio.com/products/clc-genomics-workbench). *Drosophila*
555 *melanogaster* reference genome (Release 6) (Hoskins et al., 2015) was used for mapping
556 in this research.

557 The transcription factor binding site enrichment and the Gene Ontology enrichment
558 analyses of the differentially expressed genes were carried out using Pscan
559 (http://159.149.160.88/pscan/) and online GO enrichment analysis (http://geneontology.
560 org/), respectively. We chose -450- 50 bases of the annotated transcription start site of
561 the genes as the transcription factor binding sites for enrichment analysis. The analysis
562 performed with the TFBSs matrices that is available in the JASPAR databases (version

563 Jaspar 2018_NR). Data were visualized through the circos software
564 http://circos.ca/software/.

565

566 **Statistics and reproducibility**

567 We did not use statistical methods to predetermine sample sizes but the sample sizes used
568 in this study are similar or higher as those used in previous studies (Proske et al., 2021;
569 Wagner *et al.*, 2021). Specific approaches to randomly allocate samples to groups were
570 not used and the experiments were not performed in a blinded design. No data were
571 excluded from the analysis. Prism (GraphPad version 7) was used for statistical analyses
572 and the corresponding tests used are listed in the figure legends.

573

574 Acknowledgments

575 **Funding**

576 This work was funded by the DFG as part of the CRC 1182 and by funding of the CLSM
577 (INST 257/591-1 FUGG). Moreover, Xiao Niu received funds from the Chinese Scholarship
578 Council and Weifang Medical University. Leizhi Shi received funds from the Linyi People's
579 Hospital.

580

581 **References**

582

583 Adnot, S., Lipskaia, L., and Bernard, D. (2019). The STATus of STAT3 in Lung Cell Senescence? Am J Respir
584 Cell Mol Biol *61*, 5-6. 10.1165/rcmb.2019-0013ED.
585 Andrew, D.J., and Ewald, A.J. (2010). Morphogenesis of epithelial tubes: Insights into tube formation,
586 elongation, and elaboration. Dev Biol *341*, 34-55. 10.1016/j.ydbio.2009.09.024.
587 Arbouzova, N.I., and Zeidler, M.P. (2006). JAK/STAT signalling in Drosophila: insights into conserved
588 regulatory and cellular functions. Development *133*, 2605-2616. 10.1242/dev.02411.
589 Athari, S.S. (2019). Targeting cell signaling in allergic asthma. Signal Transduct Target Ther *4*, 45.
590 10.1038/s41392-019-0079-0.
591 Bach, E.A., Ekas, L.A., Ayala-Camargo, A., Flaherty, M.S., Lee, H., Perrimon, N., and Baeg, G.H. (2007). GFP
592 reporters detect the activation of the Drosophila JAK/STAT pathway in vivo. Gene Expr Patterns *7*, 323-331.
593 10.1016/j.modgep.2006.08.003.
594 Baligar, P., Pokhrel, S., and Mukhopadhyay, A. (2016). Experimental Liver Fibrosis and Intrasplenic
595 Transplantation of CD45+ Bone Marrow Cells. Bio-protocol *6*, e1972. 10.21769/BioProtoc.1972.
596 Bergman, P., Seyedoleslami Esfahani, S., and Engstrom, Y. (2017). Drosophila as a Model for Human
597 Diseases-Focus on Innate Immunity in Barrier Epithelia. Curr Top Dev Biol *121*, 29-81.
598 10.1016/bs.ctdb.2016.07.002.
599 Bonnelykke, K., Sleiman, P., Nielsen, K., Kreiner-Moller, E., Mercader, J.M., Belgrave, D., den Dekker, H.T.,
600 Husby, A., Sevelsted, A., Faura-Tellez, G., et al. (2014). A genome-wide association study identifies CDHR3
601 as a susceptibility locus for early childhood asthma with severe exacerbations. Nat Genet *46*, 51-55.
602 10.1038/ng.2830.
603 Bosch, J.A., Tran, N.H., and Hariharan, I.K. (2015). CoinFLP: a system for efficient mosaic screening and for
604 visualizing clonal boundaries in Drosophila. Development *142*, 597-606. 10.1242/dev.114603.
605 Bossen, J., Uliczka, K., Steen, L., Neugebauer, P., Mai, M.M., Fink, C., Stracke, F., Heine, H., and Roeder, T.
606 (2021). Driver mutations in major lung cancer oncogenes can be analyzed in Drosophila models. ALTEX *38*,
607 235-244. 10.14573/altex.1912131.
608 Bossen, J., Uliczka, K., Steen, L., Pfefferkorn, R., Mai, M.M., Burkhardt, L., Spohn, M., Bruchhaus, I., Fink, C.,
609 Heine, H., and Roeder, T. (2019). An EGFR-Induced Drosophila Lung Tumor Model Identifies Alternative
610 Combination Treatments. Mol Cancer Ther *18*, 1659-1668. 10.1158/1535-7163.MCT-19-0168.
611 Brand, A.H., and Perrimon, N. (1993). Targeted gene expression as a means of altering cell fates and
612 generating dominant phenotypes. Development *118*, 401-415.
613 Brown, S., Hu, N., and Hombria, J.C. (2001). Identification of the first invertebrate interleukin JAK/STAT
614 receptor, the Drosophila gene domeless. Curr Biol *11*, 1700-1705. 10.1016/s0960-9822(01)00524-3.
615 Campos-Ortega, J.A., and Hartenstein, V. (1997). The Embryonic Development of Drosophila melanogaster
616 (Springer-Verlag Berlin Heidelberg). 10.1007/978-3-662-22489-2.
617 Chen, F., and Krasnow, M.A. (2014). Progenitor outgrowth from the niche in Drosophila trachea is guided
618 by FGF from decaying branches. Science *343*, 186-189. 10.1126/science.1241442.

619 Chen, X., Miao, M., Zhou, M., Chen, J., Li, D., Zhang, L., Sun, A., Guan, M., Wang, Z., Liu, P., et al. (2021).
620 Poly-L-arginine promotes asthma angiogenesis through induction of FGFBP1 in airway epithelial cells via
621 activation of the mTORC1-STAT3 pathway. Cell Death Dis *12*, 761. 10.1038/s41419-021-04055-2.
622 Choi, S.M., McAleer, J.P., Zheng, M., Pociask, D.A., Kaplan, M.H., Qin, S., Reinhart, T.A., and Kolls, J.K.
623 (2013). Innate Stat3-mediated induction of the antimicrobial protein Reg3gamma is required for host
624 defense against MRSA pneumonia. J Exp Med *210*, 551-561. 10.1084/jem.20120260.
625 D'Amico, S., Shi, J., Martin, B.L., Crawford, H.C., Petrenko, O., and Reich, N.C. (2018). STAT3 is a master
626 regulator of epithelial identity and KRAS-driven tumorigenesis. Genes Dev *32*, 1175-1187.
627 10.1101/gad.311852.118.
628 Daubeuf, F., and Frossard, N. (2013). Acute Asthma Models to Ovalbumin in the Mouse. Curr Protoc
629 Mouse Biol *3*, 31-37. 10.1002/9780470942390.mo120202.
630 Dutta, P., Sabri, N., Li, J., and Li, W.X. (2014). Role of STAT3 in lung cancer. JAKSTAT *3*, e999503.
631 10.1080/21623996.2014.999503.
632 Fahy, J.V., and Dickey, B.F. (2010). Airway mucus function and dysfunction. N Engl J Med *363*, 2233-2247.
633 10.1056/NEJMra0910061.
634 Fink, C., Hoffmann, J., Knop, M., Li, Y., Isermann, K., and Roeder, T. (2016). Intestinal FoxO signaling is
635 required to survive oral infection in Drosophila. Mucosal Immunol *9*, 927-936. 10.1038/mi.2015.112.
636 Gao, H., Guo, R.F., Speyer, C.L., Reuben, J., Neff, T.A., Hoesel, L.M., Riedemann, N.C., McClintock, S.D.,
637 Sarma, J.V., Van Rooijen, N., et al. (2004). Stat3 activation in acute lung injury. J Immunol *172*, 7703-7712.
638 10.4049/jimmunol.172.12.7703.
639 Georas, S.N., Donohue, P., Connolly, M., and Wechsler, M.E. (2021). JAK inhibitors for asthma. J Allergy Clin
640 Immunol *148*, 953-963. 10.1016/j.jaci.2021.08.013.
641 Georas, S.N., and Rezaee, F. (2014). Epithelial barrier function: at the front line of asthma immunology and
642 allergic airway inflammation. J Allergy Clin Immunol *134*, 509-520. 10.1016/j.jaci.2014.05.049.
643 Giridhar, P.V., Bell, S.M., Sridharan, A., Rajavelu, P., Kitzmiller, J.A., Na, C.L., Kofron, M., Brandt, E.B.,
644 Ericksen, M., Naren, A.P., et al. (2016). Airway Epithelial KIF3A Regulates Th2 Responses to Aeroallergens. J
645 Immunol *197*, 4228-4239. 10.4049/jimmunol.1600926.
646 Glasheen, B.M., Robbins, R.M., Piette, C., Beitel, G.J., and Page-McCaw, A. (2010). A matrix
647 metalloproteinase mediates airway remodeling in Drosophila. Dev Biol *344*, 772-783.
648 10.1016/j.ydbio.2010.05.504.
649 Gon, Y., and Hashimoto, S. (2018). Role of airway epithelial barrier dysfunction in pathogenesis of asthma.
650 Allergol Int *67*, 12-17. 10.1016/j.alit.2017.08.011.
651 Guha, A., Lin, L., and Kornberg, T.B. (2008). Organ renewal and cell divisions by differentiated cells in
652 Drosophila. Proc Natl Acad Sci U S A *105*, 10832-10836. 10.1073/pnas.0805111105.
653 Harrison, D.A., Binari, R., Nahreini, T.S., Gilman, M., and Perrimon, N. (1995). Activation of a Drosophila
654 Janus kinase (JAK) causes hematopoietic neoplasia and developmental defects. EMBO J *14*, 2857-2865.
655 Heijink, I.H., Brandenburg, S.M., Postma, D.S., and van Oosterhout, A.J. (2012). Cigarette smoke impairs
656 airway epithelial barrier function and cell-cell contact recovery. Eur Respir J *39*, 419-428.
657 10.1183/09031936.00193810.

658 Heijink, I.H., Kuchibhotla, V.N.S., Roffel, M.P., Maes, T., Knight, D.A., Sayers, I., and Nawijn, M.C. (2020).
659 Epithelial cell dysfunction, a major driver of asthma development. Allergy *75*, 1902-1917.
660 10.1111/all.14421.
661 Hokuto, I., Ikegami, M., Yoshida, M., Takeda, K., Akira, S., Perl, A.K., Hull, W.M., Wert, S.E., and Whitsett,
662 J.A. (2004). Stat-3 is required for pulmonary homeostasis during hyperoxia. J Clin Invest *113*, 28-37.
663 10.1172/JCI19491.
664 Hombria, J.C., and Sotillos, S. (2013). JAK-STAT pathway in Drosophila morphogenesis: From organ selector
665 to cell behavior regulator. JAKSTAT *2*, e26089. 10.4161/jkst.26089.
666 Hoskins, R.A., Carlson, J.W., Wan, K.H., Park, S., Mendez, I., Galle, S.E., Booth, B.W., Pfeiffer, B.D., George,
667 R.A., Svirskas, R., et al. (2015). The Release 6 reference sequence of the Drosophila melanogaster genome.
668 Genome Res *25*, 445-458. 10.1101/gr.185579.114.
669 Hu, X., Li, J., Fu, M., Zhao, X., and Wang, W. (2021). The JAK/STAT signaling pathway: from bench to clinic.
670 Signal Transduct Target Ther *6*, 402. 10.1038/s41392-021-00791-1.
671 Isaac, D.D., and Andrew, D.J. (1996). Tubulogenesis in Drosophila: a requirement for the trachealess gene
672 product. Genes Dev *10*, 103-117. 10.1101/gad.10.1.103.
673 Jayaram, S.A., Senti, K.A., Tiklova, K., Tsarouhas, V., Hemphala, J., and Samakovlis, C. (2008). COPI vesicle
674 transport is a common requirement for tube expansion in Drosophila. PLoS One *3*, e1964.
675 10.1371/journal.pone.0001964.
676 Jeon, M., Nguyen, H., Bahri, S., and Zinn, K. (2008). Redundancy and compensation in axon guidance:
677 genetic analysis of the Drosophila Ptp10D/Ptp4E receptor tyrosine phosphatase subfamily. Neural Dev *3*,
678 3. 10.1186/1749-8104-3-3.
679 Jiang, H., Patel, P.H., Kohlmaier, A., Grenley, M.O., McEwen, D.G., and Edgar, B.A. (2009). Cytokine/Jak/Stat
680 signaling mediates regeneration and homeostasis in the Drosophila midgut. Cell *137*, 1343-1355.
681 10.1016/j.cell.2009.05.014.
682 Jin, H., Ciechanowicz, A.K., Kaplan, A.R., Wang, L., Zhang, P.X., Lu, Y.C., Tobin, R.E., Tobin, B.A., Cohn, L.,
683 Zeiss, C.J., et al. (2018). Surfactant protein C dampens inflammation by decreasing JAK/STAT activation
684 during lung repair. Am J Physiol Lung Cell Mol Physiol *314*, L882-L892. 10.1152/ajplung.00418.2017.
685 Juncadella, I.J., Kadl, A., Sharma, A.K., Shim, Y.M., Hochreiter-Hufford, A., Borish, L., and Ravichandran, K.S.
686 (2013). Apoptotic cell clearance by bronchial epithelial cells critically influences airway inflammation.
687 Nature *493*, 547-551. 10.1038/nature11714.
688 Kallsen, K., Zehethofer, N., Abdelsadik, A., Lindner, B., Kabesch, M., Heine, H., and Roeder, T. (2015).
689 ORMDL deregulation increases stress responses and modulates repair pathways in Drosophila airways. J
690 Allergy Clin Immunol *136*, 1105-1108. 10.1016/j.jaci.2015.04.009.
691 Kida, H., Mucenski, M.L., Thitoff, A.R., Le Cras, T.D., Park, K.S., Ikegami, M., Muller, W., and Whitsett, J.A.
692 (2008). GP130-STAT3 regulates epithelial cell migration and is required for repair of the bronchiolar
693 epithelium. Am J Pathol *172*, 1542-1554. 10.2353/ajpath.2008.071052.
694 Kiu, H., and Nicholson, S.E. (2012). Biology and significance of the JAK/STAT signalling pathways. Growth
695 Factors *30*, 88-106. 10.3109/08977194.2012.660936.
696 Levi, B.P., Ghabrial, A.S., and Krasnow, M.A. (2006). Drosophila talin and integrin genes are required for
697 maintenance of tracheal terminal branches and luminal organization. Development *133*, 2383-2393.
698 10.1242/dev.02404.

699 Levine, B.D., and Cagan, R.L. (2016). Drosophila Lung Cancer Models Identify Trametinib plus Statin as
700 Candidate Therapeutic. Cell Rep *14*, 1477-1487. 10.1016/j.celrep.2015.12.105.
701 Lindsay, S.A., Lin, S.J.H., and Wasserman, S.A. (2018). Short-Form Bomanins Mediate Humoral Immunity in
702 Drosophila. J Innate Immun *10*, 306-314. 10.1159/000489831.
703 Liu, L., Johnson, W.A., and Welsh, M.J. (2003). Drosophila DEG/ENaC pickpocket genes are expressed in the
704 tracheal system, where they may be involved in liquid clearance. Proc Natl Acad Sci U S A *100*, 2128-2133.
705 10.1073/pnas.252785099.
706 Liu, R.Y., Zeng, Y., Lei, Z., Wang, L., Yang, H., Liu, Z., Zhao, J., and Zhang, H.T. (2014). JAK/STAT3 signaling is
707 required for TGF-beta-induced epithelial-mesenchymal transition in lung cancer cells. Int J Oncol *44*, 1643-
708 1651. 10.3892/ijo.2014.2310.
709 Lock, J.G., and Stow, J.L. (2005). Rab11 in recycling endosomes regulates the sorting and basolateral
710 transport of E-cadherin. Mol Biol Cell *16*, 1744-1755. 10.1091/mbc.e04-10-0867.
711 Loh, C.Y., Arya, A., Naema, A.F., Wong, W.F., Sethi, G., and Looi, C.Y. (2019). Signal Transducer and Activator
712 of Transcription (STATs) Proteins in Cancer and Inflammation: Functions and Therapeutic Implication. Front
713 Oncol *9*, 48. 10.3389/fonc.2019.00048.
714 Major, J., Crotta, S., Llorian, M., McCabe, T.M., Gad, H.H., Priestnall, S.L., Hartmann, R., and Wack, A.
715 (2020). Type I and III interferons disrupt lung epithelial repair during recovery from viral infection. Science
716 *369*, 712-717. 10.1126/science.abc2061.
717 Makris, S., Paulsen, M., and Johansson, C. (2017). Type I Interferons as Regulators of Lung Inflammation.
718 Front Immunol *8*, 259. 10.3389/fimmu.2017.00259.
719 Martin, M. (2011). Cutadapt Removes Adapter Sequences From High-Throughput Sequencing Reads.
720 EMBnet.journal *17*, 10-12. doi.org/10.14806/ej.17.1.200.
721 Matsuzaki, Y., Xu, Y., Ikegami, M., Besnard, V., Park, K.S., Hull, W.M., Wert, S.E., and Whitsett, J.A. (2006).
722 Stat3 is required for cytoprotection of the respiratory epithelium during adenoviral infection. J Immunol
723 *177*, 527-537. 10.4049/jimmunol.177.1.527.
724 Miguel-Aliaga, I., Jasper, H., and Lemaitre, B. (2018). Anatomy and Physiology of the Digestive Tract of
725 Drosophila melanogaster. Genetics *210*, 357-396. 10.1534/genetics.118.300224.
726 Milara, J., Ballester, B., Morell, A., Ortiz, J.L., Escriva, J., Fernandez, E., Perez-Vizcaino, F., Cogolludo, A.,
727 Pastor, E., Artigues, E., et al. (2018). JAK2 mediates lung fibrosis, pulmonary vascular remodelling and
728 hypertension in idiopathic pulmonary fibrosis: an experimental study. Thorax *73*, 519-529.
729 10.1136/thoraxjnl-2017-210728.
730 Morris, R., Kershaw, N.J., and Babon, J.J. (2018). The molecular details of cytokine signaling via the
731 JAK/STAT pathway. Protein Sci *27*, 1984-2009. 10.1002/pro.3519.
732 Nogueira-Silva, C., Santos, M., Baptista, M.J., Moura, R.S., and Correia-Pinto, J. (2006). IL-6 is constitutively
733 expressed during lung morphogenesis and enhances fetal lung explant branching. Pediatr Res *60*, 530-536.
734 10.1203/01.pdr.0000242300.09427.3b.
735 Oshima, K., and Fehon, R.G. (2011). Analysis of protein dynamics within the septate junction reveals a
736 highly stable core protein complex that does not include the basolateral polarity protein Discs large. J Cell
737 Sci *124*, 2861-2871. 10.1242/jcs.087700.
738 Pandey, U.B., and Nichols, C.D. (2011). Human disease models in Drosophila melanogaster and the role of
739 the fly in therapeutic drug discovery. Pharmacol Rev *63*, 411-436. 10.1124/pr.110.003293.

740 Parakh, S., Ernst, M., and Poh, A.R. (2021). Multicellular Effects of STAT3 in Non-small Cell Lung Cancer:
741 Mechanistic Insights and Therapeutic Opportunities. Cancers (Basel) *13*. 10.3390/cancers13246228.
742 Paris, A.J., Hayer, K.E., Oved, J.H., Avgousti, D.C., Toulmin, S.A., Zepp, J.A., Zacharias, W.J., Katzen, J.B.,
743 Basil, M.C., Kremp, M.M., et al. (2020). STAT3-BDNF-TrkB signalling promotes alveolar epithelial
744 regeneration after lung injury. Nat Cell Biol *22*, 1197-1210. 10.1038/s41556-020-0569-x.
745 Perrimon, N., and Mahowald, A.P. (1986). l(1)hopscotch, A larval-pupal zygotic lethal with a specific
746 maternal effect on segmentation in Drosophila. Dev Biol *118*, 28-41. 10.1016/0012-1606(86)90070-9.
747 Philips, R.L., Wang, Y., Cheon, H., Kanno, Y., Gadina, M., Sartorelli, V., Horvath, C.M., Darnell, J.E., Jr., Stark,
748 G.R., and O'Shea, J.J. (2022). The JAK-STAT pathway at 30: Much learned, much more to do. Cell *185*, 3857-
749 3876. 10.1016/j.cell.2022.09.023.
750 Piairo, P., Moura, R.S., Baptista, M.J., Correia-Pinto, J., and Nogueira-Silva, C. (2018). STATs in Lung
751 Development: Distinct Early and Late Expression, Growth Modulation and Signaling Dysregulation in
752 Congenital Diaphragmatic Hernia. Cell Physiol Biochem *45*, 1-14. 10.1159/000486218.
753 Powers, N., and Srivastava, A. (2019). JAK/STAT signaling is involved in air sac primordium development of
754 Drosophila melanogaster. FEBS Lett *593*, 658-669. 10.1002/1873-3468.13355.
755 Prange, R., Thiedmann, M., Bhandari, A., Mishra, N., Sinha, A., Hasler, R., Rosenstiel, P., Uliczka, K., Wagner,
756 C., Yildirim, A.O., et al. (2018). A Drosophila model of cigarette smoke induced COPD identifies Nrf2
757 signaling as an expedient target for intervention. Aging (Albany NY) *10*, 2122-2135.
758 10.18632/aging.101536.
759 Prele, C.M., Yao, E., O'Donoghue, R.J., Mutsaers, S.E., and Knight, D.A. (2012). STAT3: a central mediator of
760 pulmonary fibrosis? Proc Am Thorac Soc *9*, 177-182. 10.1513/pats.201201-007AW.
761 Proske, A., Bossen, J., von Frieling, J., and Roeder, T. (2021). Low-protein diet applied as part of
762 combination therapy or stand-alone normalizes lifespan and tumor proliferation in a model of intestinal
763 cancer. Aging (Albany NY) *13*, 24017-24036. 10.18632/aging.203692.
764 Quinton, L.J., and Mizgerd, J.P. (2011). NF-kappaB and STAT3 signaling hubs for lung innate immunity. Cell
765 Tissue Res *343*, 153-165. 10.1007/s00441-010-1044-y.
766 Rawlings, J.S., Rosler, K.M., and Harrison, D.A. (2004). The JAK/STAT signaling pathway. J Cell Sci *117*, 1281-
767 1283. 10.1242/jcs.00963.
768 Roeder, T., Isermann, K., and Kabesch, M. (2009). Drosophila in asthma research. Am J Respir Crit Care
769 Med *179*, 979-983. 10.1164/rccm.200811-1777PP.
770 Roeder, T., Isermann, K., Kallsen, K., Uliczka, K., and Wagner, C. (2012). A Drosophila asthma model - what
771 the fly tells us about inflammatory diseases of the lung. Adv Exp Med Biol *710*, 37-47. 10.1007/978-1-
772 4419-5638-5_5.
773 Roskoski, R., Jr. (2016). Janus kinase (JAK) inhibitors in the treatment of inflammatory and neoplastic
774 diseases. Pharmacol Res *111*, 784-803. 10.1016/j.phrs.2016.07.038.
775 Sato, M., Kitada, Y., and Tabata, T. (2008). Larval cells become imaginal cells under the control of
776 homothorax prior to metamorphosis in the Drosophila tracheal system. Dev Biol *318*, 247-257.
777 10.1016/j.ydbio.2008.03.025.
778 Severgnini, M., Takahashi, S., Rozo, L.M., Homer, R.J., Kuhn, C., Jhung, J.W., Perides, G., Steer, M., Hassoun,
779 P.M., Fanburg, B.L., et al. (2004). Activation of the STAT pathway in acute lung injury. Am J Physiol Lung Cell
780 Mol Physiol *286*, L1282-1292. 10.1152/ajplung.00349.2003.

Shiga, Y., M., T.M., and Hayashi, S. (1996). A nuclear GFP/β－galactosidase fusion protein as a marker for morphogenesis in living Drosophila. Development, Growth & Differentiation *38*, 99-106. doi.org/10.1046/j.1440-169X.1996.00012.x.

Simeone-Penney, M.C., Severgnini, M., Tu, P., Homer, R.J., Mariani, T.J., Cohn, L., and Simon, A.R. (2007). Airway epithelial STAT3 is required for allergic inflammation in a murine model of asthma. J Immunol *178*, 6191-6199. 10.4049/jimmunol.178.10.6191.

Song, L., Rawal, B., Nemeth, J.A., and Haura, E.B. (2011). JAK1 activates STAT3 activity in non-small-cell lung cancer cells and IL-6 neutralizing antibodies can suppress JAK1-STAT3 signaling. Mol Cancer Ther *10*, 481-494. 10.1158/1535-7163.MCT-10-0502.

Tadokoro, T., Wang, Y., Barak, L.S., Bai, Y., Randell, S.H., and Hogan, B.L. (2014). IL-6/STAT3 promotes regeneration of airway ciliated cells from basal stem cells. Proc Natl Acad Sci U S A *111*, E3641-3649. 10.1073/pnas.1409781111.

Tsarouhas, V., Senti, K.A., Jayaram, S.A., Tiklova, K., Hemphala, J., Adler, J., and Samakovlis, C. (2007). Sequential pulses of apical epithelial secretion and endocytosis drive airway maturation in Drosophila. Dev Cell *13*, 214-225. 10.1016/j.devcel.2007.06.008.

Villarino, A.V., Kanno, Y., and O'Shea, J.J. (2017). Mechanisms and consequences of Jak-STAT signaling in the immune system. Nat Immunol *18*, 374-384. 10.1038/ni.3691.

Wagner, C., Isermann, K., and Roeder, T. (2009). Infection induces a survival program and local remodeling in the airway epithelium of the fly. FASEB J *23*, 2045-2054. 10.1096/fj.08-114223.

Wagner, C., Uliczka, K., Bossen, J., Niu, X., Fink, C., Thiedmann, M., Knop, M., Vock, C., Abdelsadik, A., Zissler, U.M., et al. (2021). Constitutive immune activity promotes JNK- and FoxO-dependent remodeling of Drosophila airways. Cell Rep *35*, 108956. 10.1016/j.celrep.2021.108956.

Weaver, M., and Krasnow, M.A. (2008). Dual origin of tissue-specific progenitor cells in Drosophila tracheal remodeling. Science *321*, 1496-1499. 10.1126/science.1158712.

Xiao, C., Puddicombe, S.M., Field, S., Haywood, J., Broughton-Head, V., Puxeddu, I., Haitchi, H.M., Vernon-Wilson, E., Sammut, D., Bedke, N., et al. (2011). Defective epithelial barrier function in asthma. J Allergy Clin Immunol *128*, 549-556 e541-512. 10.1016/j.jaci.2011.05.038.

Yew-Booth, L., Birrell, M.A., Lau, M.S., Baker, K., Jones, V., Kilty, I., and Belvisi, M.G. (2015). JAK-STAT pathway activation in COPD. Eur Respir J *46*, 843-845. 10.1183/09031936.00228414.

Zeidler, M.P., and Bausek, N. (2013). The Drosophila JAK-STAT pathway. JAKSTAT *2*, e25353. 10.4161/jkst.25353.

Zhang, X., Yue, P., Page, B.D., Li, T., Zhao, W., Namanja, A.T., Paladino, D., Zhao, J., Chen, Y., Gunning, P.T., and Turkson, J. (2012). Orally bioavailable small-molecule inhibitor of transcription factor Stat3 regresses human breast and lung cancer xenografts. Proc Natl Acad Sci U S A *109*, 9623-9628. 10.1073/pnas.1121606109.

Zheng, X.J., Yang, Z.X., Dong, Y.J., Zhang, G.Y., Sun, M.F., An, X.K., Pan, L.H., and Zhang, S.L. (2016). Downregulation of leptin inhibits growth and induces apoptosis of lung cancer cells via the Notch and JAK/STAT3 signaling pathways. Biol Open *5*, 794-800. 10.1242/bio.017798.

821 Table 1 Genes that were highly upregulated in response to *Hop.CA* overexpression.

| Name | Maximum group mean | Fold change | FDR p-value |
|---|---|---|---|
| CG16772 | 11.85 | 135.44 | 0 |
| hop | 286.06 | 35.43 | 0 |
| CG14570 | 42.21 | 35.37 | 0 |
| CG14147 | 55.31 | 32.88 | 0 |
| Hsp70Bb | 161.51 | 29.99 | 0 |
| Ubx | 200.46 | 23.51 | 0 |
| pre-mod(mdg4)-I | 1.12 | 18.67 | 2.22648E-06 |
| IM14 | 11.46 | 15.14 | 3.80132E-07 |
| IM4 | 26.43 | 14.97 | 1.74645E-12 |
| CG14569 | 1576.88 | 14.73 | 0 |
| IM2 | 7.26 | 14.47 | 2.01792E-06 |
| CG5791 | 1.79 | 13.80 | 2.90502E-05 |
| CG9121 | 3.41 | 11.54 | 0 |
| IM1 | 7.16 | 10.97 | 7.52122E-05 |
| CG11413 | 35.70 | 10.64 | 3.44242E-07 |
| CG16710 | 2.13 | 10.32 | 1.72352E-07 |
| CG31960 | 267.26 | 10.05 | 0 |
| CG16789 | 1.45 | 9.46 | 5.58576E-09 |
| CG6034 | 6.92 | 8.47 | 4.7943E-11 |
| Ace | 2.06 | 8.19 | 0 |
| CG13059 | 9.90 | 7.58 | 1.33893E-06 |
| CG31809 | 8.64 | 7.39 | 0 |
| CG7203 | 9.41 | 7.21 | 8.66989E-09 |
| Vha14-2 | 2.51 | 7.05 | 2.31024E-07 |
| wb | 7.35 | 6.69 | 0 |
| Drs | 8166.47 | 6.64 | 0 |
| CG5778 | 3.20 | 6.61 | 0.000294835 |
| CG3457 | 2.69 | 6.34 | 2.38755E-06 |
| Lcp65Ad | 9.93 | 5.79 | 2.58249E-08 |
| lectin-22C | 29.06 | 5.67 | 6.88538E-06 |
| fuss | 3.97 | 5.67 | 0 |
| CG43333 | 2.39 | 5.63 | 1.48392E-09 |
| CG18336 | 2.96 | 5.49 | 5.52167E-05 |

| | | | |
|---|---|---|---|
| CG32563 | 3.06 | 5.35 | 0.000696584 |
| FASN2 | 1.65 | 5.34 | 2.95545E-10 |
| Cyp4d21 | 45.70 | 5.31 | 0 |
| Obp57d | 1.80 | 5.28 | 0.000102926 |
| CG17560 | 2.31 | 5.22 | 0.000766701 |
| CG5888 | 68.16 | 5.20 | 0 |

822 $p < 1\times10^{-4}$, fold change > 5, maximum group mean > 1. The list is restricted to 39 genes.

823

824 Table 2 Transcription factor-binding site motifs enriched in 41 highly upregulated genes.

| Matrix ID | Matrix name | P-value |
|---|---|---|
| MA0023.1 | dl (var.2) | 0.000443261 |
| MA0022.1 | dl | 0.00407113 |
| MA0532.1 | STAT92E | 0.00794732 |
| MA0450.1 | hkb | 0.00811969 |
| MA0197.2 | nub | 0.0154201 |
| MA0242.1 | Bgb::run | 0.0371696 |
| MA0204.1 | Six4 | 0.0443521 |
| MA0444.1 | CG34031 | 0.0488169 |

825 A total of 133 transcription factor profiles were used.

826

827

828

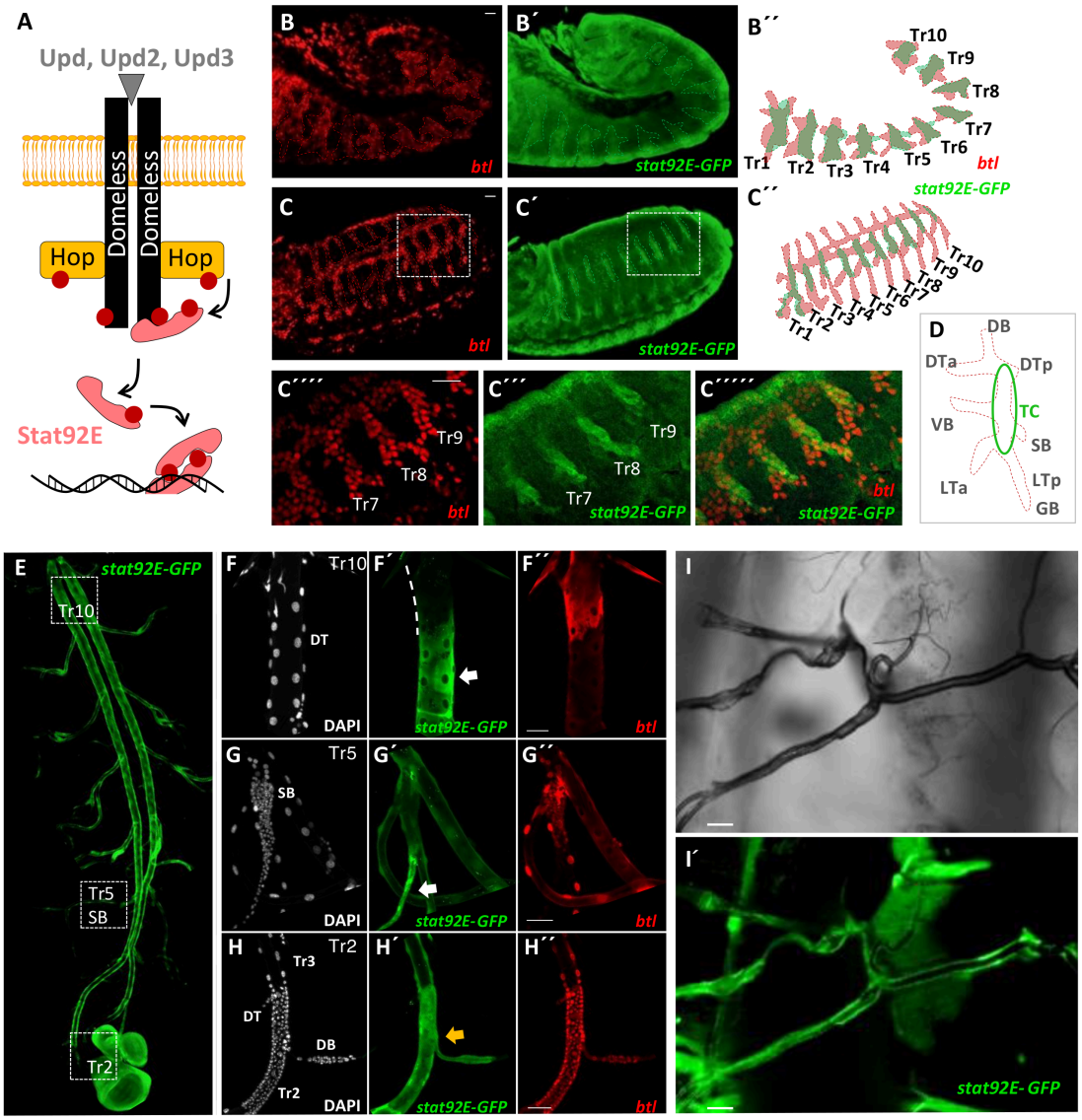


Figure 1: The activation of JAK/STAT signaling pathway in the respiratory system of *Drosophila*. (A) shows a model of JAK/STAT signaling pathway in *Drosophila* comprising all major components. Three ligands (Upd, Upd2 and Upd3) bind to a single receptor, Domeless (Dome), which transmits this information via a single JAK (Hopscotch (Hop)) to a single STAT transcription factor (STAT92E). The activation of JAK/STAT signaling through all developmental stages was detected by using a *STAT92E-GFP* reporter (*btl-Gal4*, *STAT92E-GFP*; *UAS-LacZ.nls*). (B-D) Fluorescence micrographs of embryonic trachea stained for GFP (green, JAK/STAT pathway activated zones), and beta-galactosidase (red, tracheal metamere (Tr)), respectively. The activation of JAK/STAT pathway in the terminal regions is weaker than that in the central regions before (B) and after the fuse of tracheal invaginations of all segments (C). (D) shows the activation pattern of JAK/STAT signaling in the embryonic trachea metamere. The stronger signal in the central region mainly belongs to TC (green circle). DB, dorsal

branch; DTa, dorsal trunk anterior; DTp, dorsal trunk posterior; VB, visceral branch; LTa, lateral trunk anterior; LTp, lateral trunk posterior; and GB, ganglionic branch; SB, spiracular branch; transverse connective, TC. The stronger signal in the central regions mainly belongs to TC. Scale bar: 20 µm. (E-H) Fluorescence micrographs of larval trachea. JAK/STAT activity is present in most parts of the trachea (E). The region in the posterior region of the trachea (dorsal trunk (DT) of Tr10, white dash line in F) showed a decreased activity of JAK/STAT signaling compared to other tracheal epithelial cells. Scale bar: 50 µm. Conversely, some regions like SB (G, marked by white arrow) and Tr2, DB (H, marked by white arrow) showed an increased activity of JAK/STAT signaling compared to the tracheal epithelial cells. Scale bar: 50 µm. (I) Fluorescence micrographs of adult trachea. JAK/STAT signaling was induced in the trachea of the adult.

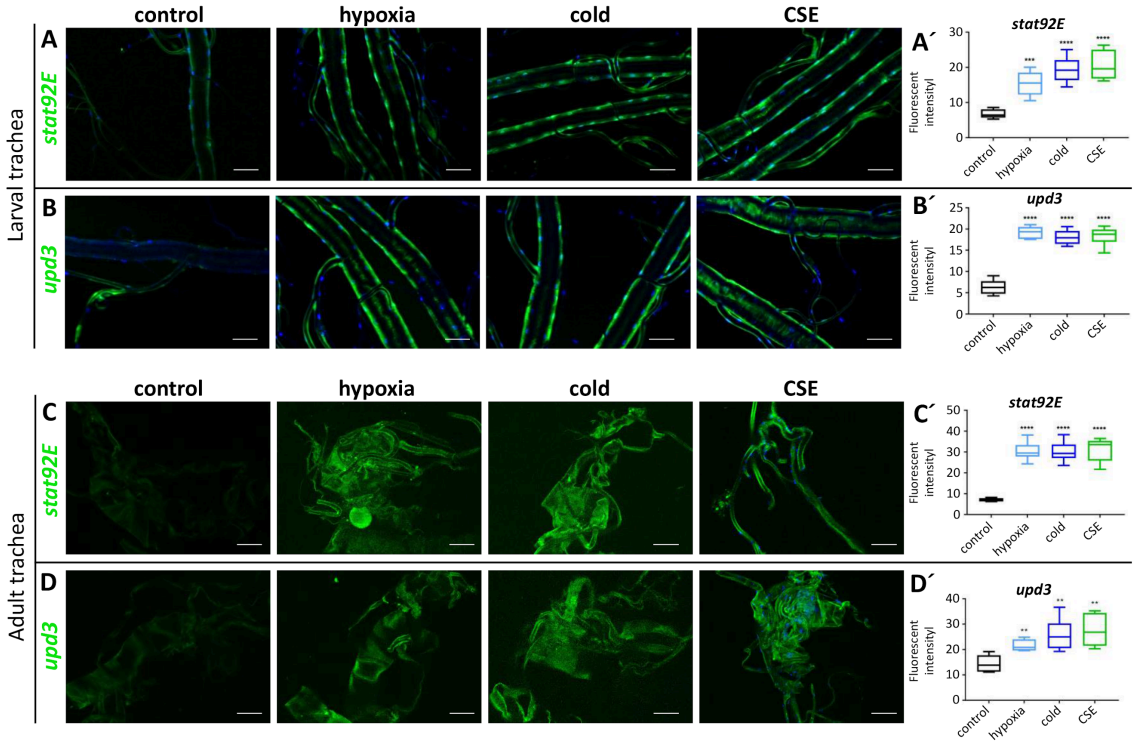


853

854 Figure 2: JAK/STAT signaling pathway in trachea was activated by external stimuli. (A and C)
855 Fluorescence micrographs of the trachea of *STAT92E-GFP* larvae (A) and adult (C) under normal
856 conditions and external stimuli, including hypoxia, cold air (cold), cigarette smoke exposure (CSE). The
857 external stimuli induced activity of STAT92E could be observed and was quantified through fluorescent
858 intensity (A' and C'). (B and D) Fluorescence micrographs of the trachea of *upd3-Gal4*; *UAS-GFP* larvae
859 (B) and adult (D) that were exposed to normal condition and external stimuli. The external stimuli
860 induced expression of *upd3* could be observed and was quantified through fluorescent intensity (B'
861 and D'). ** $p < 0.01$, *** $p < 0.001$, **** $p < 0.0001$ by Student's t-test. Scale bar: 100 µm.

862

863

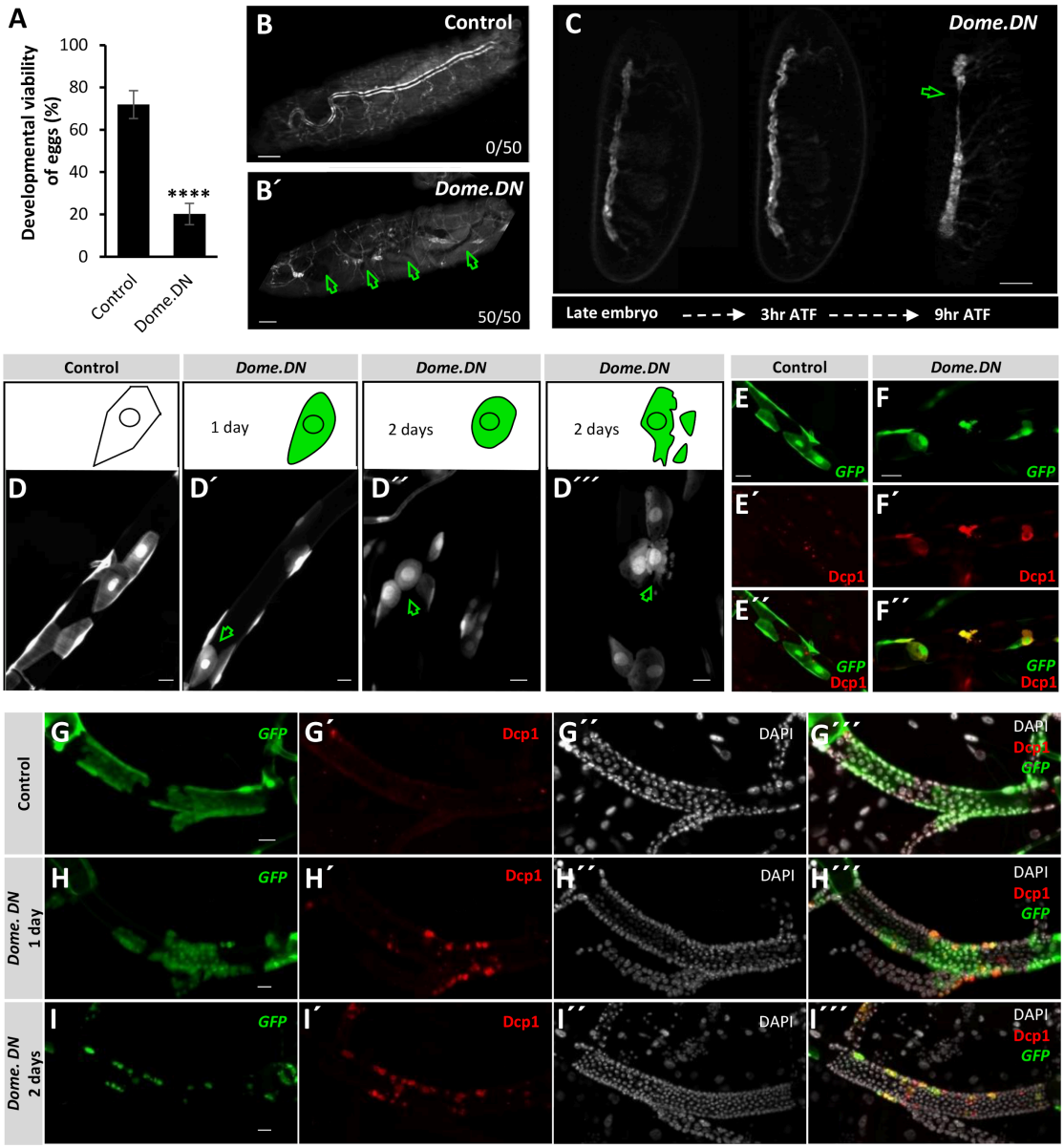


Figure 3: Inhibition of JAK/STAT signaling pathway induced epithelial cell apoptosis. (A) Ectopic blocking of JAK/STAT signaling in the trachea was done by expressing *Dome.DN* under the control of *btl-Gal4*. The developmental viability is shown by the percentage of embryos that hatched. (**** $p < 0.0001$ by Student's t-test). (B) Micrographs of surviving larvae. Scale bar: 50 µm. *Dome.DN* expression inhibited the formation of an intact tracheal tree. X/XX: emerged phenotype/total animals. (C) Time-lapse imaging of the trachea of *btl-Gal4>Dome.DN* embryos continuously for 9 hours after tracheal formation (9hr ATF). Scale bar: 50 µm. (D-I) Fluorescence micrographs of *Dome.DN* expressing mosaic mutant clones (GFP, green) in the larval trachea (*vvl-FLP*, *CoinFLP-Gal4, UAS-EGFP; tub-Gal80[ts]* (*vvl-coin.ts*)*>Dome.DN*). (D) Negative regulation of JAK/STAT pathway by expressing *Dome.DN* in the trachea led to changes in cell morphology (D' and D'') and disintegration afterwards (D''', green arrows, Scale

875 bar: 20 µm). (E-F) Fluorescence micrographs of the tracheal somatic cells of *vvl-coin.ts* larvae (E), and
876 the tracheal somatic cells of *vvl-coin.ts>Dome.DN* larvae (F) stained for cleaved Dcp1 (red, on day 2
877 after induction). Scale bar: 50 µm. (G-I) The progenitor cells of Tr2 could be stained by cleaved Dcp1
878 earlier than the mutant somatic cells (red, on day 1 after induction). Scale bar: 50 µm. Nuclei are
879 stained with DAPI.

880

881

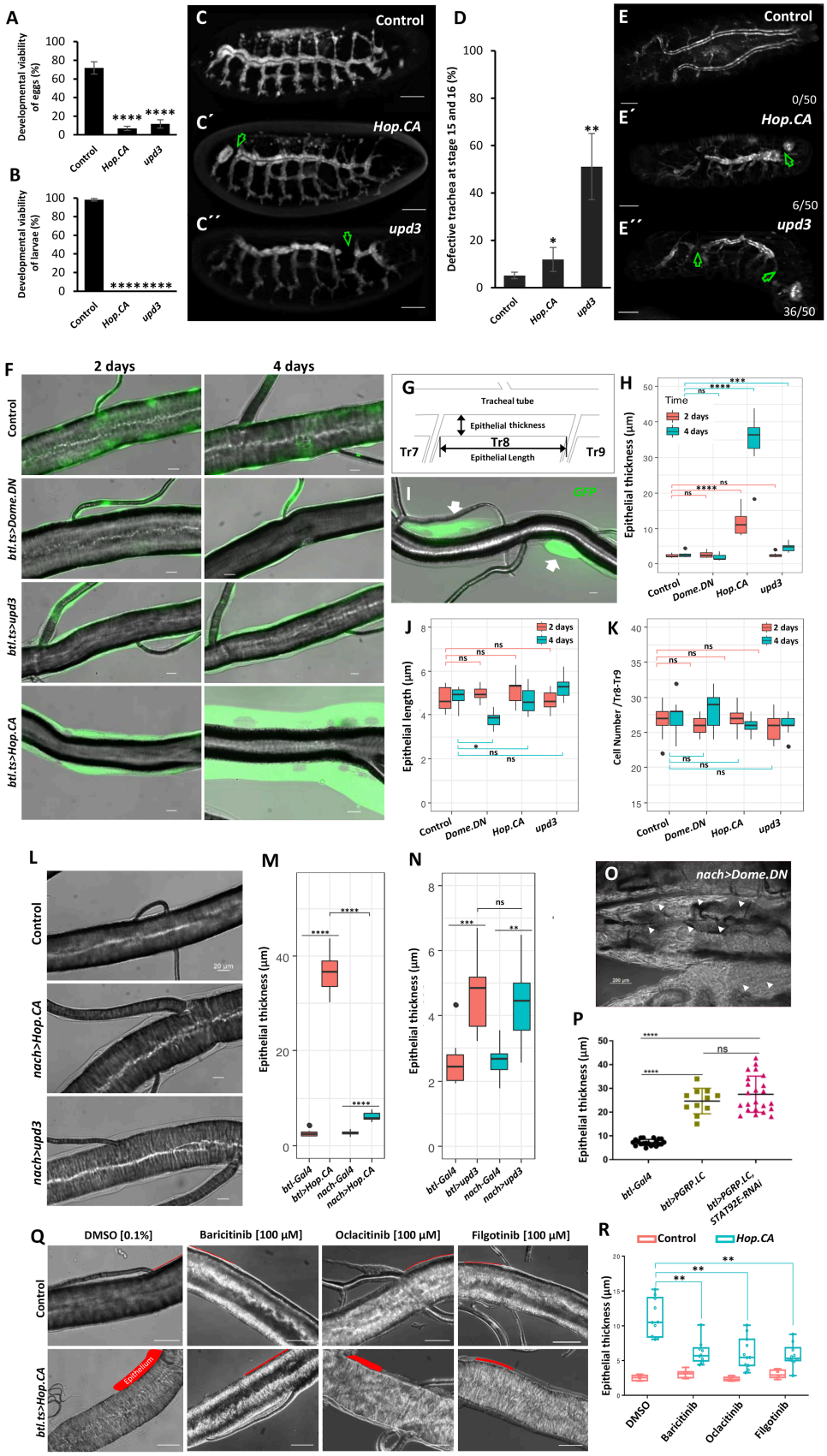
A
Developmental viability of eggs (%)
Control
Hop.CA
upd3
B
Developmental viability of larvae (%)
C
Control
C´
Hop.CA
C´´
upd3
D
Defective trachea at stage 15 and 16 (%)
E
Control
0/50
E´
Hop.CA
6/50
E´´
upd3
36/50
F
2 days
4 days
Control
btl.ts>Dome.DN
btl.ts>upd3
btl.ts>Hop.CA
G
Tracheal tube
Epithelial thickness
Tr7
Tr8
Tr9
Epithelial Length
I
GFP
H
Time
2 days
4 days
Epithelial thickness (µm)
Control
Dome.DN
Hop.CA
upd3
J
Epithelial length (µm)
K
Cell Number /Tr8-Tr9
L
Control
nach>Hop.CA
nach>upd3
M
Epithelial thickness (µm)
btl-Gal4
btl>Hop.CA
nach-Gal4
nach>Hop.CA
N
btl>upd3
nach>upd3
O
nach>Dome.DN
P
btl-Gal4
btl>PGRP.LC
btl>PGRP.LC, STAT92E-RNAi
Q
DMSO [0.1%]
Baricitinib [100 µM]
Oclacitinib [100 µM]
Filgotinib [100 µM]
Control
btl.ts>Hop.CA
Epithelium
R
Control
Hop.CA
DMSO
Baricitinib
Oclacitinib
Filgotinib

882

Figure 4: Ectopic activation of JAK/STAT signaling in the trachea induced cell thickening. Ectopic regulation of JAK/STAT signaling in the trachea was performed by expressing *Hop.CA* or *upd3* for activation and *Dome.DN* for inhibition of the pathway, under the control of *btl-Gal4*. The percentage of embryos that hatched (A) and the percentage of larvae that developed into pupa (B) are shown. (C) Fluorescence micrographs of *btl>Hop.CA* (or *btl>upd3*) embryos. Scale bar: 50 µm. (D-E) Activation of the JAK/STAT pathway in the trachea led to uncompleted tracheal development during tracheal morphogenesis. (D) Quantification of the numbers of defect trachea in *btl>Hop.CA* or *btl>upd3* embryos. (E) Micrographs of the trachea of the surviving larvae. Scale bar: 50 µm. (F) Ectopic activation of epithelial JAK/STAT signaling (*Hop.CA* or *upd3*) or inactivation (*Dome.DN*) under control of *btl.ts-Gal4* (dorsal trunk of Tr8 of L3 larvae). Larvae were raised at 29 ℃ for 2 or 4 days for induction, respectively. Scale bar: 20 µm. (G) Illustration of epithelial thickness, epithelial length. (H) Statistical analysis of the epithelial thicknesses in DT8 of the corresponding larvae. (I) Micrographs of DT8 of *vvl-FLP*, *CoinFLP-Gal4, UAS-EGFP* (*vvl-coin*)*>Hop.CA* larvae. Scale bar: 20 µm. The thickening of the tracheal epithelium is observed in those cells that express *Hop.CA* (arrows). (J-K) Quantification of epithelial length and the cell number of the DT8 region of larvae with different types of ectopic manipulation (including *Dome.DN*, *Hop.CA* and *upd3* expression in the trachea driven by *btl-Gal4, tubPGal80ts*) for 2 or 4 days, respectively. Mild activation of epithelial JAK/STAT signaling mitigated the thickening phenotype. (L) Micrographs of the DT8 regions of *nach-Gal4* larvae, *nach>Hop.CA* larvae and *nach>upd3* larvae. Scale bar: 20 µm. (M-N) Quantification of the epithelial thickness of the DT8 region of those larvae whose JAK/STAT signaling were activated by expressing *Hop.CA* or *upd3* under the control of *nach-Gal4* and *btl-Gal4*. (O) Micrographs of *nach>Dome.DN* larvae experiencing suppression of the JAK/STAT pathway make trachea translucent and filled with fluids. Triangle indicates the tracheal position. Scale bar: 200 µm. (P) Quantification of the epithelial thickness of the DT8 region of *btl-Gal4* larvae, *btl>PGRP.LC* larvae and *btl>PGRP.LC, STAT92E-RNAi* larvae. *TubPGal80ts* was used to inhibit the expression of *UAS-PGRP.LC* and *UAS-STAT92E*$^{RNAi}$ before animal become L3 larvae and activated *UAS-* genes expression for one day. Changes in epithelial thickness could be rescued by application of specific JAK inhibitors (Q and R). (Q) Microscopy of the tracheal epithelium (L3 larvae). Control crossings *btl-Gal4, tubPGal80ts>w*$^{1118}$ compared to JAK/STAT activated crossings *btl-Gal4, tubPGal80ts>Hop.CA.* Scale bar: 50 µm. (R) Quantification of epithelial thickness (highlighted in red) of the JAK inhibitors (Baricitinib, Oclacitinib, Filgotinib) compared to DMSO control. Green arrow: the defective region, ns means no significant, * $p < 0.05$, ** $p < 0.01$, *** $p < 0.001$, **** $p < 0.0001$ by Student's t-test.

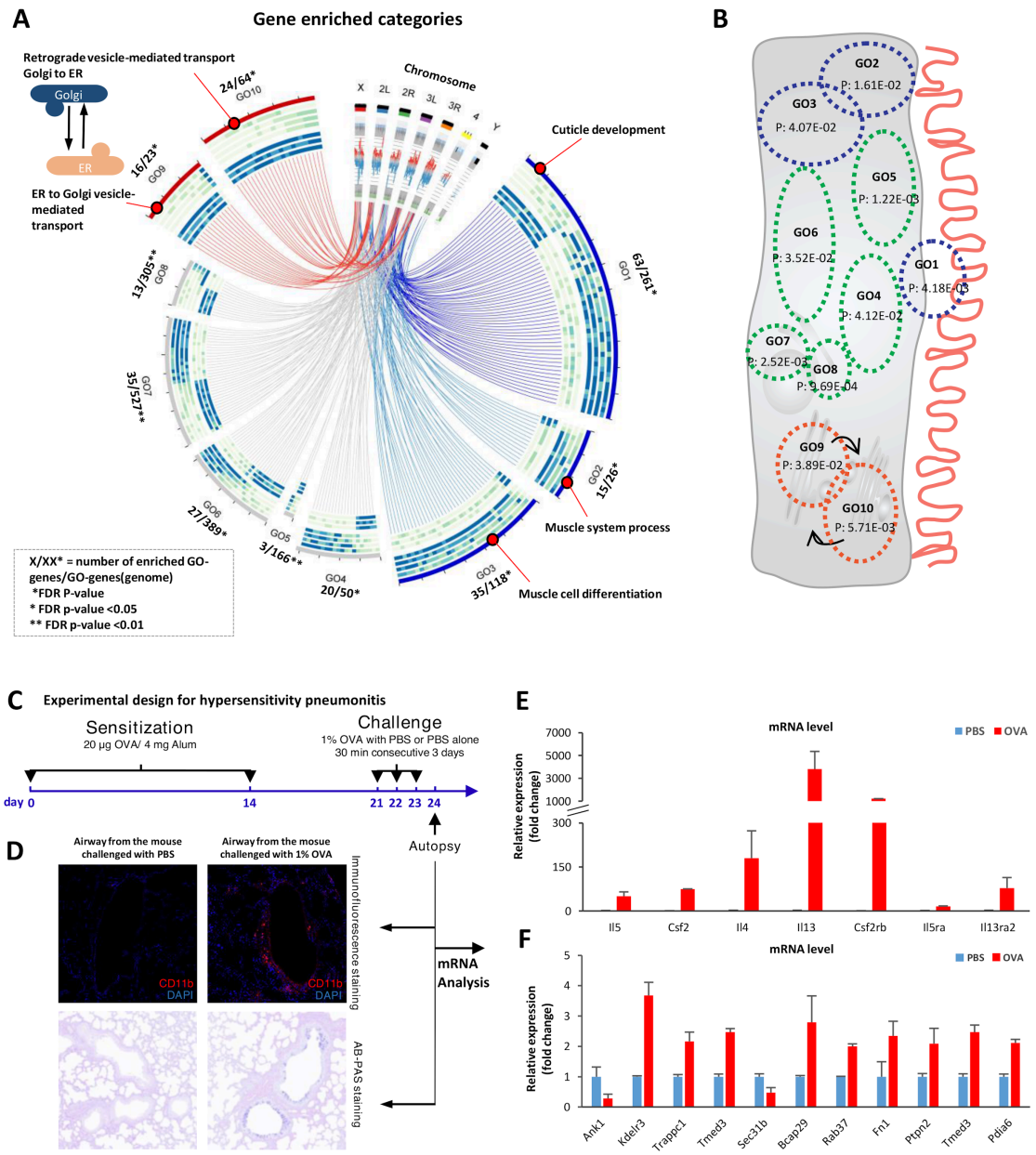


Figure 5: Gene Ontology (GO) enrichment analysis of the 2004 annotated differentially expressed genes in *Hop.CA* overexpressing airways *vs*. controls. (A) Gene ontology analysis showed 10 biological processes that were enriched in *Hop.CA* overexpressing airways compared with matching controls. Most regulated genes in the GO1, GO2, and GO3 were downregulated. Most regulated genes that involved in the COPI-and COPII-mediated vesicular transport between endoplasmic reticulum and Golgi (GO9 and GO10) were up-regulated. GO1, cuticle development; GO2, muscle system process; GO3, muscle cell differentiation; GO4, glutathione metabolic process; GO5, detection of chemical stimulus; GO6, cellular protein-containing complex assembly; GO7, RNA processing; GO8, translation; GO9, endoplasmic reticulum to Golgi vesicle-mediated transport; GO10, retrograde vesicle-mediated

transport Golgi to the endoplasmic reticulum. (B) Enriched biological processes were superimposed on a sketch depicting a tracheal epithelial cell, with the corresponding *p*-value added. Blue indicates processes where genes were mainly down-regulated; red indicates processes where genes were mainly up-regulated; green indicates processes where genes were both down-regulated and up-regulated to similar extents. (C) Experimental design for the OVA induced asthma model. Mice were sensitized with intraperitoneal injections of 20 μg of OVA emulsified in aluminum hydroxide in a total volume of 1 ml on days 7 and 14, followed by 3 consecutive challenges each day by exposure to OVA or PBS aerosol for 30 min. Mice were sacrificed 24 h following the final challenge. The left lungs were collected for histological analysis and the superior lobes were dissected for RNA analysis. (D) The lungs were stained with CD11b antibody and with the standard Alcian blue (AB) method followed by the Periodic acid–Schiff (PAS) technique. (E) Important chemokines and chemokine receptors induced by OVA aerosol are involved in JAK/STAT signaling pathway. (F) The genes that function in the process of ER to Golgi vesicle-mediated transport are mostly upregulated when the mice were exposed to OVA aerosol.

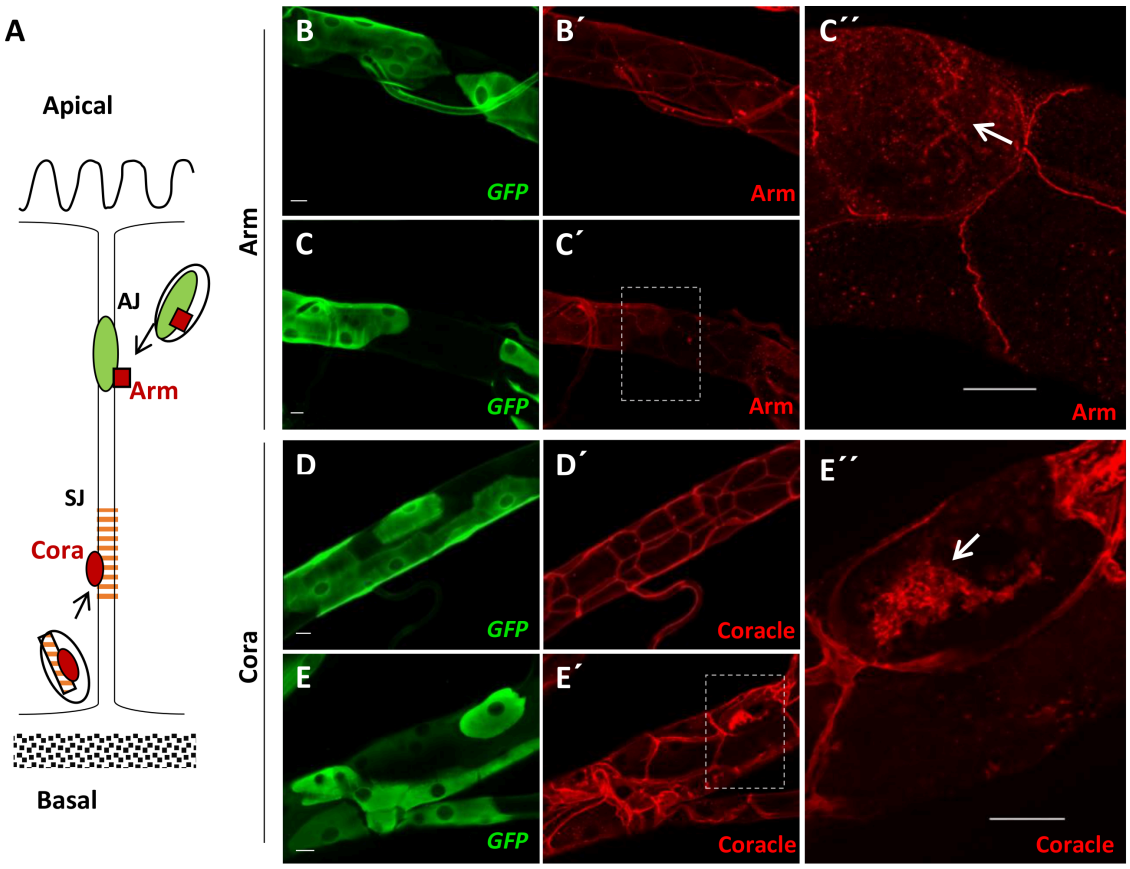


941

942 Figure 6: Activation of airway epithelial JAK/STAT signaling affects vesicle-mediated transport of
943 proteins. (A) Schematic orientation of Arm and Cora at the contact zone between two airway epithelial
944 cells. Adherens junction (AJ), septate junction (SJ). Trachea of *vvl-coin* larvae (control; B and D) and *vvl-*
945 *coin>Hop.CA* larvae (treatment; C and E) stained for GFP (green, Gal4 positive cells), Arm or Cora (red),
946 respectively. 30 specimens were investigated in each group. Scale bar: 20 µm.

947

948

949

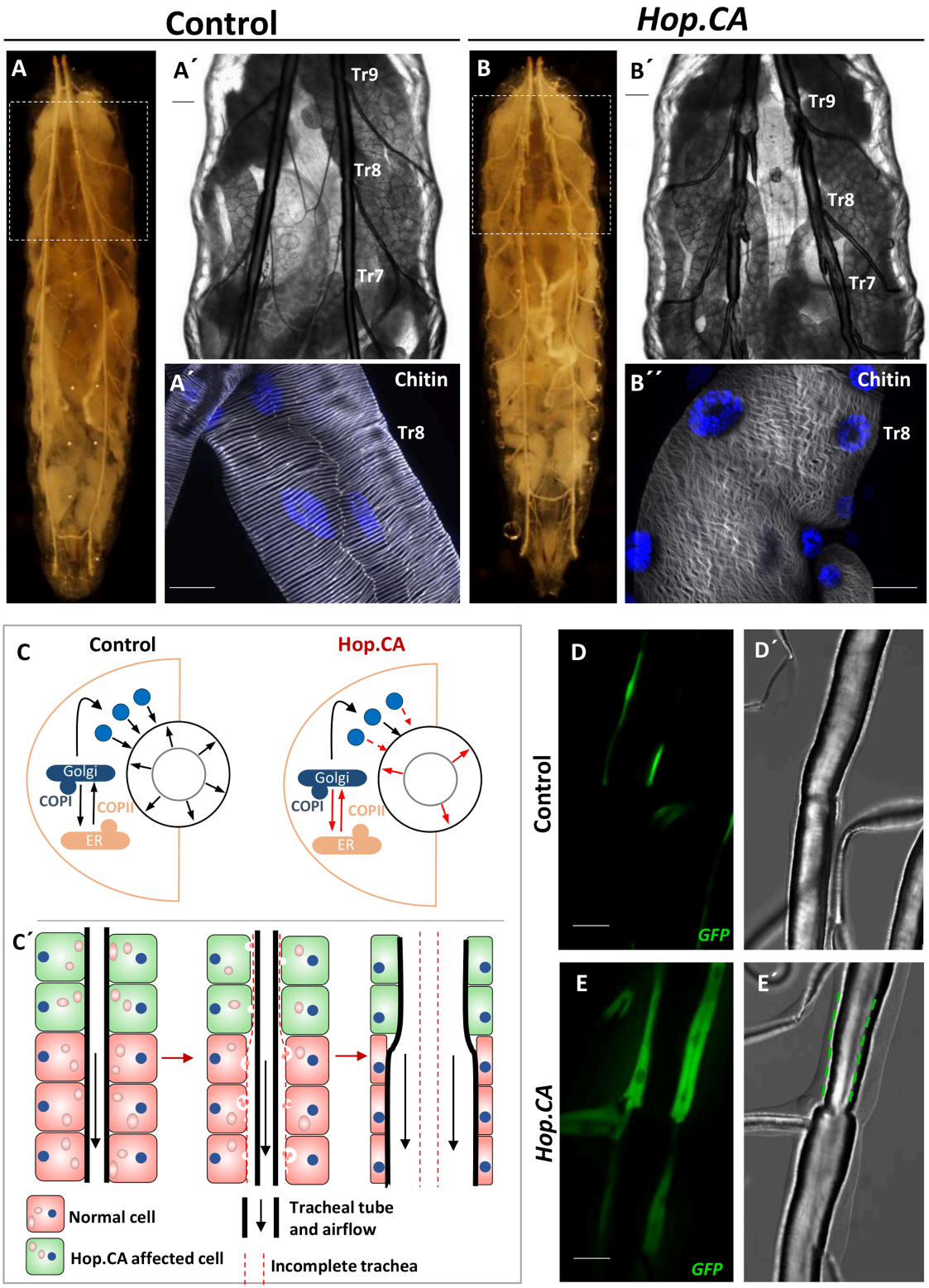
Control
Hop.CA
A
A´
Tr9
Tr8
Tr7
A´´
Chitin
Tr8
B
B´
Tr9
Tr8
Tr7
B´´
Chitin
Tr8
C
Control
Hop.CA
Golgi
COPI
COPII
ER
C´
Normal cell
Hop.CA affected cell
Tracheal tube and airflow
Incomplete trachea
D
D´
E
E´
Control
Hop.CA
GFP
GFP

950

951 Figure 7: Activation of JAK/STAT signaling in airway epithelial cells affects the development of the
952 epicuticle. (A-B) Activation of JAK/STAT signaling in airway epithelia observed in whole larvae by
953 expressing *UAS-Hop.CA* under the control of the *btl.ts* (B-B'') compared to the control (A-A''). In (A'
954 and B') the region containing Tr7-Tr9 is shown. (A'' and B'') Chitin staining of isolated airways (at the
955 Tr8 region). Scale bar: 50 µm. (C) Schematic illustration of a potential explanation for the thickening of
956 the epithelium and narrowing of the tube. In the control epithelium, a secretory burst of luminal
957 proteins drives the diametric expansion of the tubes, and this process depends on vesicle-mediated
958 transport. COPI-and COPII-mediated vesicular transport plays a central role in this process, mutation
959 members in the process underly the tube size defect in previous reports (Jayaram et al., 2008;
960 Tsarouhas et al., 2007). Although active JAK induced the expression of the genes involved in the vesicle-
961 mediated transport, long-term activation eventually impedes the transport of vesicles out of the cell
962 (C). This dysfunction of transport could lead to the appearance of tube size defects such as the increase
963 in the cell volume and narrowing of the tube size (C') (Jayaram et al., 2008; Tsarouhas et al., 2007). (D-
964 E) Micrographs of the trachea of *vvl-coin* larvae (control; D) and *vvl-coin>Hop.CA* larvae (treatment; E).
965 Cells with *vvl-Gal* expression are stained with GFP (D-E). The green dash line in the E' show stenosis in
966 the regions with cells expressing *Hop.CA* to a high degree. Scale bar: 50 µm.

967

968